Copyright Warning & Restrictions

The copyright law of the United States (Title 17, United States Code) governs the making of photocopies or other reproductions of copyrighted material.

Under certain conditions specified in the law, libraries and archives are authorized to furnish a photocopy or other reproduction. One of these specified conditions is that the photocopy or reproduction is not to be "used for any purpose other than private study, scholarship, or research." If a, user makes a request for, or later uses, a photocopy or reproduction for purposes in excess of "fair use" that user may be liable for copyright infringement,

This institution reserves the right to refuse to accept a copying order if, in its judgment, fulfillment of the order would involve violation of copyright law.

Please Note: The author retains the copyright while the New Jersey Institute of Technology reserves the right to distribute this thesis or dissertation

Printing note: If you do not wish to print this page, then select "Pages from: first page # to: last page #" on the print dialog screen

ABSTRACT

DESIGN AND AUTOMATED OPERATION OF A CONDENSATION-INDUCED DEPRESSURIZATION SYSTEM

by
Fen Du

Typical examples of the use of the vacuum environments in industry include vacuum coating, vacuum drying, vacuum packing, vacuum casting, vacuum heat treatment, vacuum cooling for food storage and leakage detection. Most of these applications require a comparatively small volume of vacuum environment. However, there are also many applications where enormous vacuum chambers are needed. For example, a large vacuum chamber is used to simulate the conditions of space.

This study investigates the design and the automated operation of a vacuum generation system based on the idea of the condensation-induced depressurization with prefilled condensable medium in a confined, adiabatic chamber. The operation process of this new system includes mainly four phases, steam filling phase, cooling phase, usage phase and transition phase, operating sequentially. An automated control system based on these phases is designed and implemented on a laboratory scaled experimental system. This experimental system serves as a vacuum environment application to demonstrate the automatic and continuous operation of the condensation-induced depressurization system. In order to obtain a better understanding on the selection of parameters for performance improvement, models of the first three process phases are developed and analyzed. These models provide a reference for the design of systems for other industry applications as well.

Methods of improving the system design and operation are investigated. The analysis shows that high pressure and fast flow steam source will accelerate the steam filling process. Removal of the transition phase improves the steam filling phase and speeds up the vacuum preparation. Improvement can also be achieved on the coordination between vacuum generation and usage through control elements, as well as the proper selection of volume ratio between usage chamber and preparation chambers.

The ultimate objective of this study is that the results can be used to develop guidelines for the design and operation of vacuum generation systems according to specific usage patterns of the vacuum environment applications.

DESIGN AND AUTOMATED OPERATION OF A CONDENSATION-INDUCED DEPRESSURIZATION SYSTEM

by
Fen Du

A Dissertation
Submitted to the Faculty of
New Jersey Institute of Technology
in Partial Fulfillment of the Requirements for the Degree of
Doctor of Philosophy in Mechanical Engineering

Department of Mechanical and Industrial Engineering

May 2012

.

APPROVAL PAGE

DESIGN AND AUTOMATED OPERATION OF A CONDENSATION-INDUCED DEPRESSURIZATION SYSTEM

Fen Du

Dr. Zhiming Ji, Dissertation Co-Advisor Associate Professor of Mechanical Engineering, NJIT	Date
Dr. Chao Zhu, Dissertation Co-Advisor Professor of Mechanical Engineering, NJIT	Date
Dr. Rajpal S. Sodhi, Committee Member Professor of Mechanical Engineering, NJIT	Date
Dr. Bernard Koplik, Committee Member Professor of Mechanical Engineering, NJIT	Date
Dr. Sui-hoi E. Hou, Committee Member Associate Professor of Electrical and Computer Engineering, NJIT	Date

BIOGRAPHICAL SKETCH

Author: Fen Du

Degree: Doctor of Philosophy

Date: April 2012

Undergraduate and Graduate Education:

- Doctor of Philosophy in Mechanical Engineering,
  New Jersey Institute of Technology, Newark, NJ, 2012

- Master of Science in Physical Electronics,
  Huazhong University of Science and Technology, Wuhan, P. R. China, 2007

- Bachelor of Science in Mechanical Engineering,
  Huazhong University of Science and Technology, Wuhan, P. R. China, 2004

Major: Mechanical Engineering

Presentations and Publications:

Manna, Yazan A., Du, Fen and Ji, Zhiming, "Motion Control and Coordination in the Development of A Conceptual Gait Rehabilitation System", *the Institution of Mechanical Engineers, Part C, Journal of Mechanical Engineering Science*, In Press.

He, Pengfei, Zhu, Chao, Du, Fen, Ji, Zhiming and Lin, Chao-Hsin, "Effect of Wall Cooling with Condensation on Depressurization of a Steam-prefilled Chamber", submitted to ASME 2012 International Mechanical Engineering Congress & Exposition, Houston, Texas, November 9-15, 2012.

He, Pengfei, Zhu, Chao, Du, Fen, Ji, Zhiming and Lin, Chao-Hsin, "Condensation-induced Depressurization of Steam-prefilled Chamber", under preparation for submission to *International Journal of Heat and Mass Transfer*.

DEDICATED TO MY FAMILY

ACKNOWLEDGMENT

I would like to express my deepest appreciation to my research advisor, Dr. Zhiming Ji for his support and help through my entire study period in NJIT. He taught me many skills in work, opened my mind in research and inspired me from difficulties.

I would also like to give my deep appreciation to Dr. Chao Zhu, my research co-advisor, for his support, guidance, and suggestions for my study. His attitude always inspires me to perform better in research.

Special thanks are given to Dr. Rajpal Sodhi, Dr. Bernard Koplik and Dr. Sui-hoi E. Hou for their supports and participating in my committee.

Appreciation is also given to my university, New Jersey Institute of Technology, and Department of Mechanical and Industrial Engineering for supporting me during my study.

I also thank Dr. Dawei Wang, Dr. Rajesh Patel, Dr. Yazan A. Manna, Mr. Pengfei He and Mr. Raivat Patel for their help during my PhD study. Thanks to Mr. Joseph Glaz and Mr. Greg Policastro for their technical support.

Finally, I would like to thank my family. To my dear parents, Mr. Bangwei Du and Ms. Manying Hu, thank you for your constant encouragement which inspires me in my every step. To my dear husband, Ting Tan, thank you very much for your support and consideration.

TABLE OF CONTENTS

TABLE OF CONTENTS
(Continued)

Chapter **Page**

LIST OF TABLES

LIST OF FIGURES

LIST OF FIGURES
(Continued)

LIST OF FIGURES
(Continued)

Figure **Page**

LIST OF SYMBOLS

c_T	Specific heat of steel
c_{pa}	Constant-pressure specific heat of air
c_{va}	Constant-volume specific heat of air
c_{pv}	Constant-pressure specific heat of vapor
c_{vp}	Constant-volume specific heat of vapor
h_i	Specific enthalpy of inlet steam
h_a	Specific enthalpy of air inside the depressurization chamber
h_v	Specific enthalpy of vapor inside the depressurization chamber
h_e	Specific enthalpy of gaseous mixture (air + vapor)
m_a	Mass of air inside the depressurization chamber
m_e	Mass of the gas mixture at the exit
m_i	Mass of the steam at inlet
m_v	Mass of vapor inside the depressurization chamber
m_T	Mass of the steel tank
G	Gas specific gravity
G_a	Specific gravity of air
G_v	Specific gravity of vapor
p_{wet}	Pressure of wet steam
p_{dry}	Pressure of dry steam
p_1	Total pressure of the depressurization chamber

p_2	Pressure of the exit environment
p_a	Pressure of the air inside the depressurization chamber
p_v	Pressure of the vapor inside the depressurization chamber
p_i	Pressure of the inlet steam
R_a	Specific gas constant of air
R_v	Specific gas constant of vapor
T	Temperature of the depressurization chamber
T_i	Temperature of the inlet steam
u_a	Specific internal energy of air inside the depressurization chamber
u_v	Specific internal energy of vapor inside the depressurization chamber
V	Volume of the depressurization chamber
γ	Mass ratio of vapor to the total mass inside the depressurization chamber

CHAPTER 1

INTRODUCTION

1.1 Objective

This study investigates a vacuum generation system based on the steam condensation and the design issues associated with its automated process control. Models on different phases of the process will be built and analyzed for the future scale-up application. Methods for improving the process and control, including coordination between vacuum generation and usage, are to be explored. The objective of this study is that the result can be used to guide the design and operation of vacuum generation systems for general applications of vacuum environment in industry.

1.2 Background

There are a lot of essential applications of the vacuum environments in industry. The most widespread ones include vacuum coating [1], vacuum drying [2], vacuum packing [3,4], vacuum heat treatment [5,6], vacuum brazing [7,8] and vacuum cooling for food storage [9,10]. For example, Figure 1.1 (a) is a vacuum dryer with cylindrical chamber. It is often used for drying metallic components after they have been cleaned in water [2]. Figure 1.1 (b) shows a vacuum chamber which tests the leaks of the packages [11].

(a) (b)

Figure 1.1 Examples of industrial applications of vacuum: (a) A vacuum dryer with cylindrical chamber [2]; (b) Leaks test of a package in a vacuum chamber [11].

In 2003, the Jet Propulsion Lab of NASA built a vacuum-sealed chamber called the Micro-arcsecond Metrology Testbed (MAM) for the Space Interferometry Mission (SIM). This application of vacuum is shown in Figure 1.2(a). The sub-atomic measurements were conducted for the first time ever in this vacuum chamber which proved that the movements of stars can be measured with an astonishing degree of accuracy never before achieved in human history [12]. Professor Frank Davidson, a former MIT researcher and early member of the first English Channel Tunnel Study group, envisioned a vacuum tunnel submerged 150 to 300 feet beneath the surface of the Atlantic Ocean, and then anchored to the seafloor. By using the magnetic levitation trains in it, the top speed

could be reached to about 5000 mph [13]. With this speed, it will spend less than an hour to travel from New York to London. This futuristic application of vacuum is depicted in Figure 1.2(b).

(a) (b)

Figure 1.2 Examples of modern and futuristic applications of vacuum: (a) A vacuum chamber to simulate the space condition [12]; (b) A vacuum tunnel used for magnetic levitation trains [13].

Hypobaric environment is also reflected in the altitude effect of the aircrafts [14, 15]. Airplane cabin altitude schedule of Boeing 767 is described in Figure 10 of [15], which shows the difference between the cabin altitude and the actual altitude of the airplane.

There are two common methods to create a sub-atmospheric pressure environment (vacuum). The first method is by extracting gases from the recipient by a vacuum pump and discharging bodily into the ambient environment outside the vacuum system. The second method is by attaching the gas molecules to a cold wall or surface of recipient either by condensation or absorption [16-21].

Vacuum pumps are widely used in generating a vacuum or hypobaric chamber. According to the physical or chemical phenomena responsible for their operations, the

vacuum pumps could be classified into mechanical pumps, turbo-molecular pumps, diffusion pumps, getter or ion pump and cryogenic pump, etc [22]. Some pumps combine two or more principles to pump a wide range of gases or to pump over a wide pressure range. Due to the operating pressure ranges, there are low vacuum pumps, medium vacuum pumps and high vacuum pumps [22]. They can also be classified by either positive or non-positive displacement. A positive-displacement pump creates vacuum by isolating and compressing a constant volume of air. When the compressed air is vented out in one port, a vacuum is created at the other port where the air is drawn in. This generates relatively high vacuum, but little flow. A non-positive displacement pump uses rotating impeller blades to accelerate air and create a vacuum at the inlet port. While this type of pumps provides high flow rates, they cannot produce high levels of vacuum. Due to the moving parts inside such pumps, their operation generally produces vibration and noise.

For an altitude chamber which simulates altitude effect on the human body, the requirement for the vacuum level is low, while the need for the vacuum supply can be high because of the large volume of the chamber. And a quiet environment is preferred. The vacuum pumps may meet the requirement to provide a vacuum chamber, but a better approach is in a great need.

Almost all the vacuum pumps are powered by electricity, while the electricity is generated by the power plants, either through heat (steam supply) or nuclear energy. From the energy efficiency point of view, the energy of heat (or steam) is first transferred to electricity, and then electricity is used to make the vacuum. There is energy loss in every transferring step. For the saturated steam, the pressure decreases fast with the fall of the temperature, for example, the pressure of the saturated steam at 373 K is 101.3 kPa, and the

pressure reduces to 2.34 kPa when the steam temperature falls to the room temperature at 293 K [23]. By using this characteristic of the steam, an alternately method of condensation based depressurization is under consideration.

In comparison with vacuum technologies using pumps, the condensation approach has unique advantages. Firstly, it has high efficiency with no leakage. Secondly, the structure is simple with no moving parts. Thirdly, it operates in low cost and noiseless. And finally, it has good adaptability to scale-ups.

The objective of this research is to design and implement automated operation of an experimental condensation-induced depressurization system. An overview of the experimental system is presented in Chapter 2. The design of an automated process control for the experimental system is discussed in Chapter 3. Since the design and operation of such a system for general application demands a better understanding of the process and its control parameters, different phases of the process have been analyzed in Chapter 4. Chapter 5 discussed design guidelines of the development of systems for general applications where depressurized environments are needed. Conclusion and future works are discussed in Chapter 6.

The main contributions of this work are summarized as follows. An automated control system for the experimental system of the altitude effect study has been designed and implemented. This control system achieved the purpose of keeping the continuous operation of the system under a safe, automated and quick response condition. Models on three different phases of the process has been built and analyzed to provide insights on improved system design and operations.

CHAPTER 2

EXPERIMENTAL SYSTEM OF DEPRESSURIZATION

A laboratory-scaled experimental system is designed to realize the condensation-based depressurization. As shown in Figure 2.1. The basic principle and detail descriptions of this experimental system are presented in this chapter.

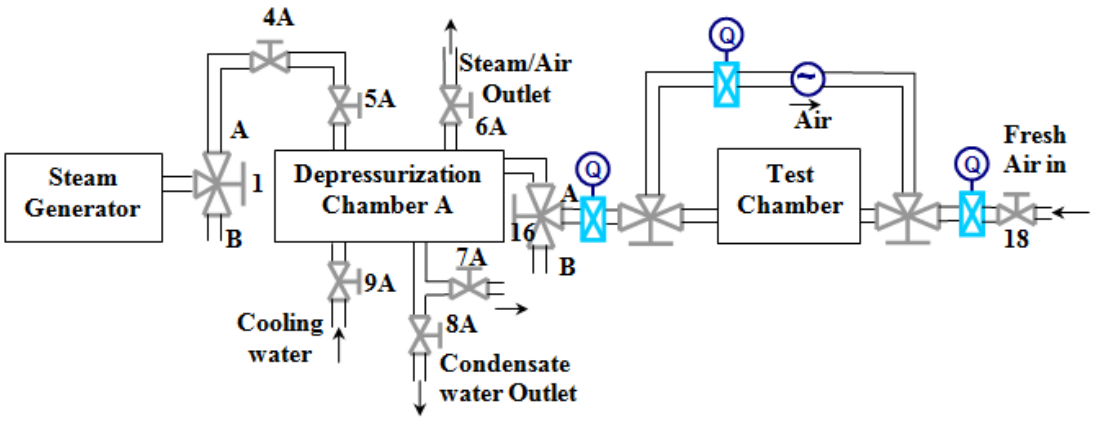

Figure 2.1 An experimental system schematic diagram with control valves locations.

2.1 Basic Principle

The basic principle of this method is to depressurize a hypobaric chamber, which is called test chamber in the experiment, by using the vacuum produced through the condensation of saturated steam vapor, or other condensable medium, in a depressurization chamber.

In this experiment system, the depressurization chamber is first fully filled with saturated steam. By cooling the depressurization chamber with a coolant, cold water is used in the experiment, the pressure in the chamber is rapidly decreased through vapor condensation to produce a vacuum environment. This generated vacuum is then used as the

vacuum supply for the test chamber. To meet the sustained vacuum supply, two depressurization chambers A and B are used so that they can take turns to prepare the vacuum for the test chamber. Only the depressurization chamber A is shown in Figure 2.1, since the design and control operation of the depressurization chamber B is the same as depressurization chamber A.

2.2 Description of the Experimental System

For the experimental system illustrated in Figure 2.1, there are mainly three parts, the steam generation, the depressurization process and the usage interface.

In the steam generation, an electrical heater is used to boil the water to provide the saturated steam. The steam supply flow rate depends on the power of the steam generator. The steam is consistently offered in order to pre-fill the depressurization chamber and maintain the continuous work of the experimental system. In the usage interface part, the test chamber is depressurized. Pressure of test chamber is stably maintained through a pressure regulator, especially a vacuum regulator, at certain hypobaric pressure, e.g., 81.060 kPa (0.8 atmosphere pressure (atm)), by using alternately vacuum generated by depressurization chambers A and B. One of the depressurization chambers is firstly prepared as it is ready to be the vacuum source. When this depressurization chamber is in use to draw air from the test chamber, the other chamber is under the process of steam filling and cooling to prepare as the next vacuum source. The two depressurization chambers are then taking turns to provide the vacuum to the test chamber. The air supply to the test chamber is made of two parts, fresh air from the outside and the circulated air from chamber itself.

The depressurization process is more complicated compare with the other two parts. A detail view of experimental set up of the depressurization chamber is shown in Figure 2.2 [23].

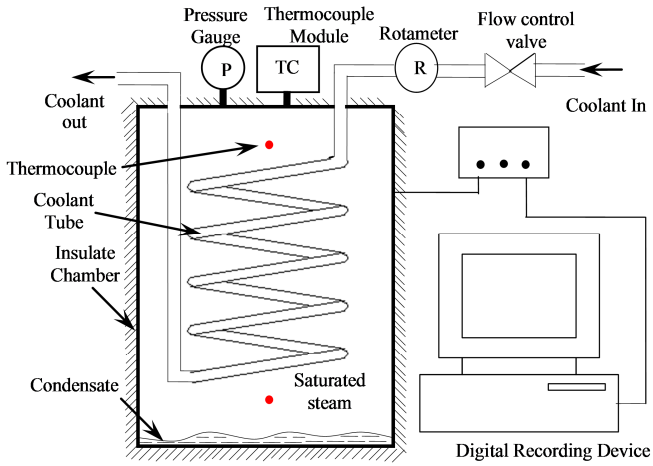

Figure 2.2 The detail view of experimental set up of the depressurization chamber.

In order to pre-fill the saturated steam, a steam-generation and non-condensable gas flushing system is used. A 30-gallon steel chamber (12.7 kg) is served as the depressurization chamber. The non-condensable gas (such as dry air) inside the chamber can be flushed out and replaced by continuous generated steam vapor after sufficient time of flushing. With pre-filled saturated steam (101.325 kPa, 373 K), without any pre-condensation, this steel chamber is initially in a thermal equilibrium with an internal cooling coil (filled with water) at a temperature of 373 K. The chamber is thermally insulated from the ambient environment. The depressurization process is conducted by continuously feeding the coolant (cold water at about 287 K) at a preset flow rate through the cooling coil located at the center of chamber, as shown in Figure 2.2. The cooling coil is

a 4.85-feet copper tube with 1/2 inch I.D., 3/8 inch-O.D. and 50 foot long copper tube. The heat-absorbed coolant is then discharged without recirculation. The condensed water remains insider the chamber throughout the entire depressurization process. Two thermocouples (type K) are located at two different locations to measure the transient temperature characteristics of the system during the depressurization process. A vacuum-pressure gauge is mounted on the chamber to measure the absolute pressure inside the chamber during depressurization process. The flow rate of cooling water is measured by a rotameter, which is located near the inlet to the chamber. A digital recording device is employed to record the transient changes in both pressure and temperature measurements during the depressurization process.

Mechanical manual valves are used in this experimental set up to control the air inlet/outlet, steam inlet/outlet, cooling water inlet and condensation water outlet, as shown in Figure 2.1. Two 3-way manual valves are used in the depressurization process. One switches the steam source to depressurization chambers A or B, the other one provide the vacuum source to the test chamber either from depressurization chamber A or B. In the test chamber usage part, a blower and another two 3-way manual valves are used to realize the air re-circulation. Since the steam is in high temperature, and the chambers are depressurized, emergency valves are also used for the safety consideration. Valves are operated based on the status of the depressurization chambers and test chamber which is monitored by the pressure gauges and thermocouples.

Experiments were conducted with this manually operated system to demonstrate the concept initially. The result shows that the pressure in the depressurization chamber can be rapidly decreased from 101.325 kPa (1 atm) to 15.200 kPa (0.15 atm) within 2

minutes or less. With this method, a predetermined depressurized environment for can be realized.

CHAPTER 3

DESIGN, IMPLEMENTATION AND OPERATION OF CONTROL SYSTEM

The experimental set up of the condensation-induced depressurization system is discussed in Chapter 2. In order to realize the automated operation of this experiment set up, the entire system is re-analyzed from the automated control point of view. The control logic is designed based on the process conditions and timing requirements. With the ladder logic diagram, the automated control system is built onto the experimental system. Experiments are conducted with this new automatic control design. The results show that the sustained automated operation of the system is achieved.

3.1 General Control Consideration of the Experimental System

The operation of the depressurized gas flow system can be divided into three major units: steam generation and its control, vacuum generation and its control and test chamber environment control, as shown in Figure 3.1.

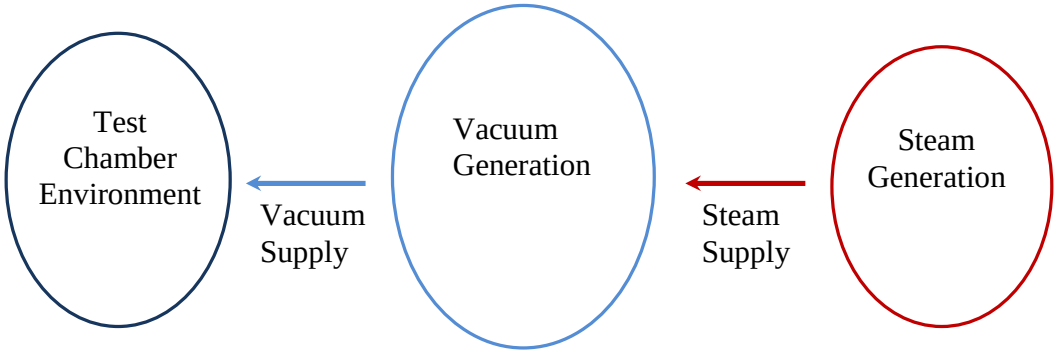

Figure 3.1 Major operation units of the experimental system.

The operation for realizing the system function effectively and safely requires coordinated control of the flow of steam, coolant and air in the system. The valves need to be opened and closed at proper time based on various conditions of the test chamber and depressurization chambers, including both pressure and temperature. It can be seen from the system schematic that more than 20 valves are used in this phase of the feasibility study. All these valves were manually operated. For this approach to become practical, a sustained automatic operation control is required. Towards this goal, the original manual-controlled system of the scale model is first analyzed and an automated control system is designed and implemented to demonstrate the continuous operation under automated process control.

All existing manual valves must be replaced by properly selected control valves. For fast response time, pneumatically actuated solenoid valves are used. For economic consideration, the two 3-way manual valves are actually replaced by two pairs of two-way pneumatically actuated valves. Other control elements needed are temperature and pressure sensors for monitoring the process conditions, as well as various timing devices.

Based on current operation requirements, the process involves only the sequential opening and closing of valves. Thus logic control is sufficient at this stage of experiment. The main goal of automatic process control is focused on vacuum generation and vacuum interface.

3.2 Logic Design for Process Timing Control

Relay controlled ladder logic diagrams are designed for current system. All original manual valves of the system are replaced with pneumatically actuated valves. The pressure and temperature indicators are also supplemented with pressure and temperature switches or transducers so that the information can be used for controlling the process.

With all the manual valves in the system being replaced with pneumatically actuated ball valves of the same size, the control system is implemented with relay logic only. Because of the time varying nature of the process, the control system is designed to operate as state based and event driven. The transitions from one state to another state of the process are detected by temperature switches and pressure switches. Latching relays are used since the actual states cannot be uniquely determined based on the ON/OFF status of these switches. By adjusting the timing settings in the opening/closing of the associated valves and/or the pressure and temperature settings in the pressure and temperature switches, the operation characteristics of the process can be modified in the future experiments. The diagrams given below show the process timing and signals from temperature and pressure switches to control the processes of cycle and process logic operation for heating and cooling system. Figures 3.2 and 3.3 showed the timing, operation sequence and process logic operations in continuous operation case. Figures 3.4 and 3.5 illustrated the timing, operation sequence and process logic operations in discontinuous operation case.

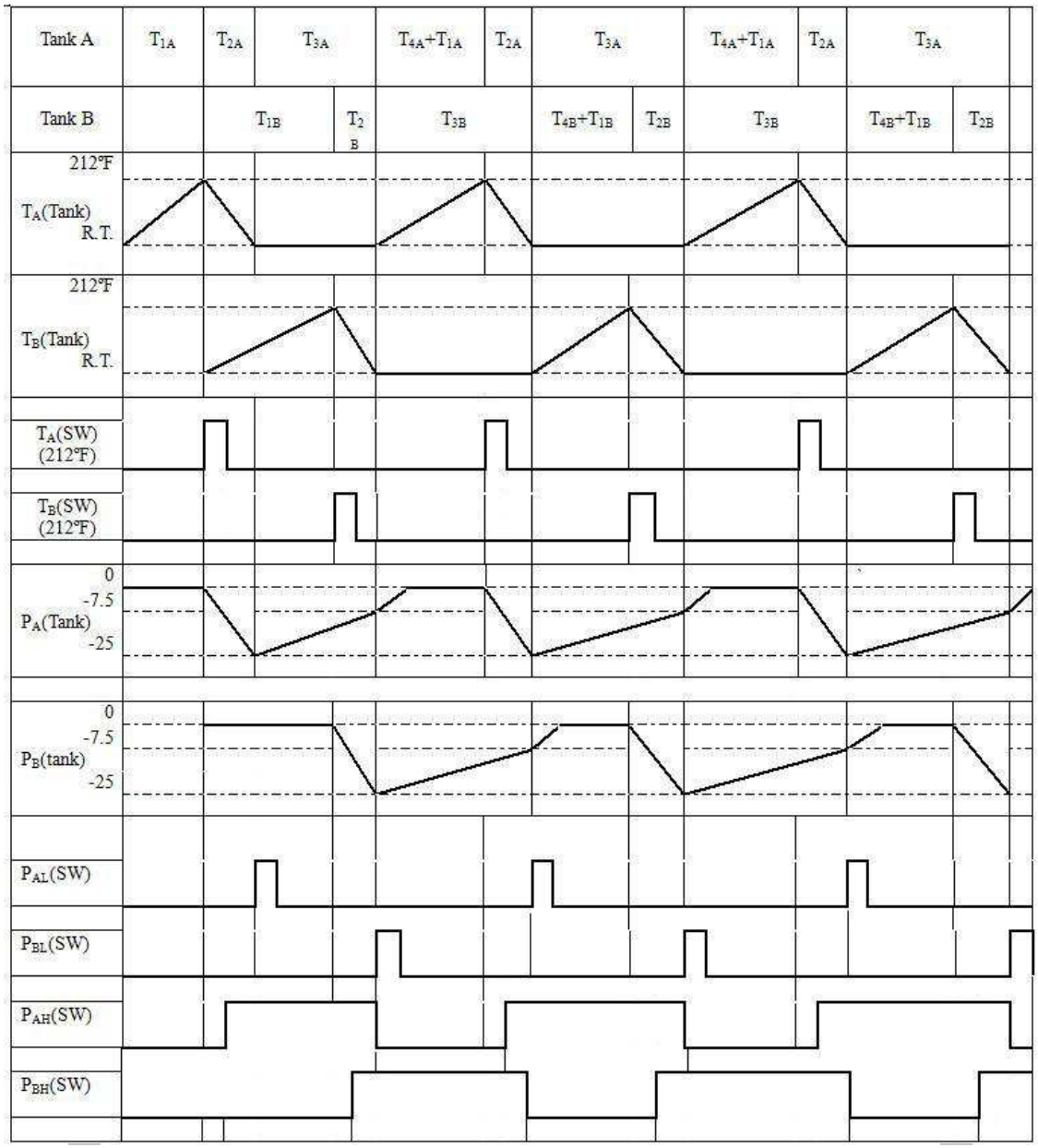

Figure 3.2 Process timing and signals from temperature and pressure switches in continuous operation case.

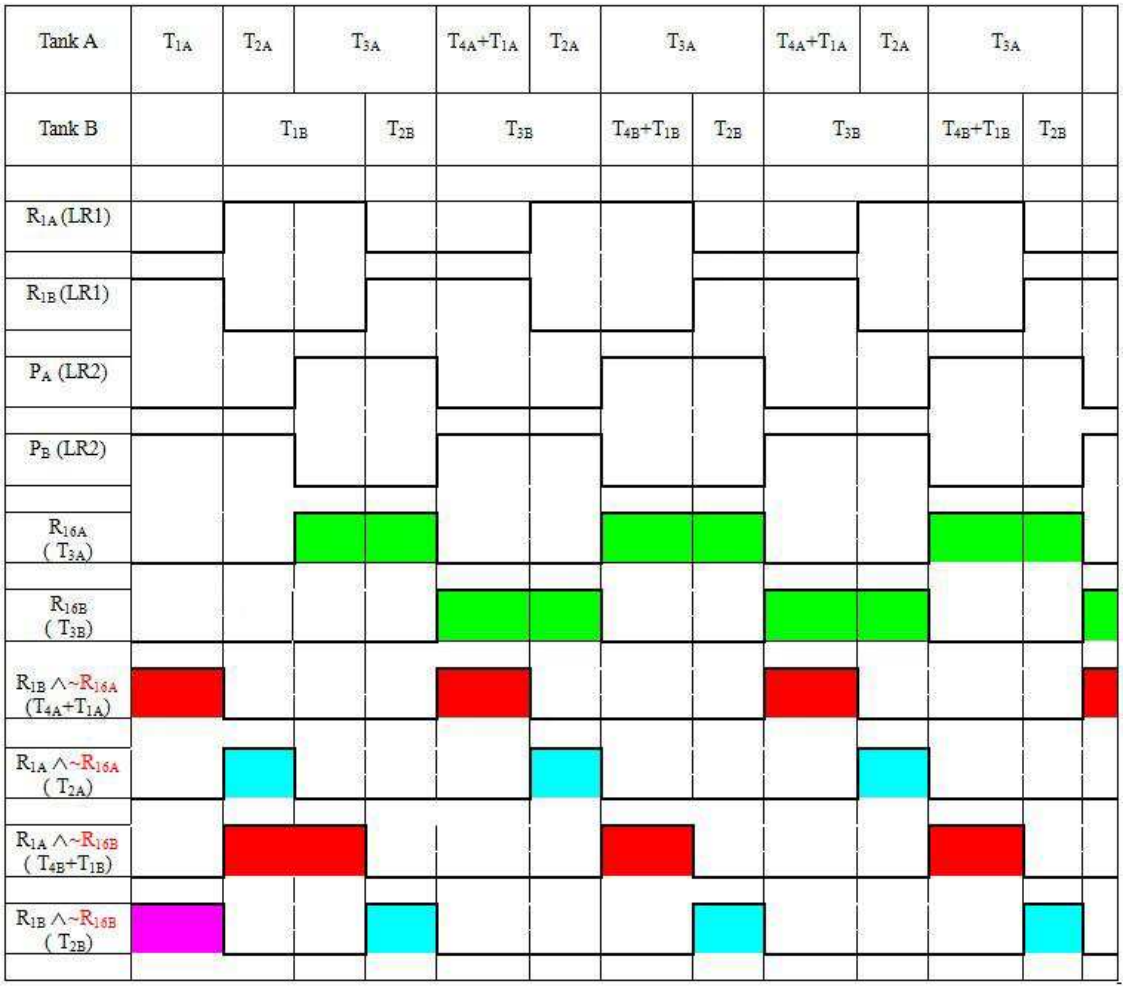

Figure 3.3 Process logic operations in continuous operation case.

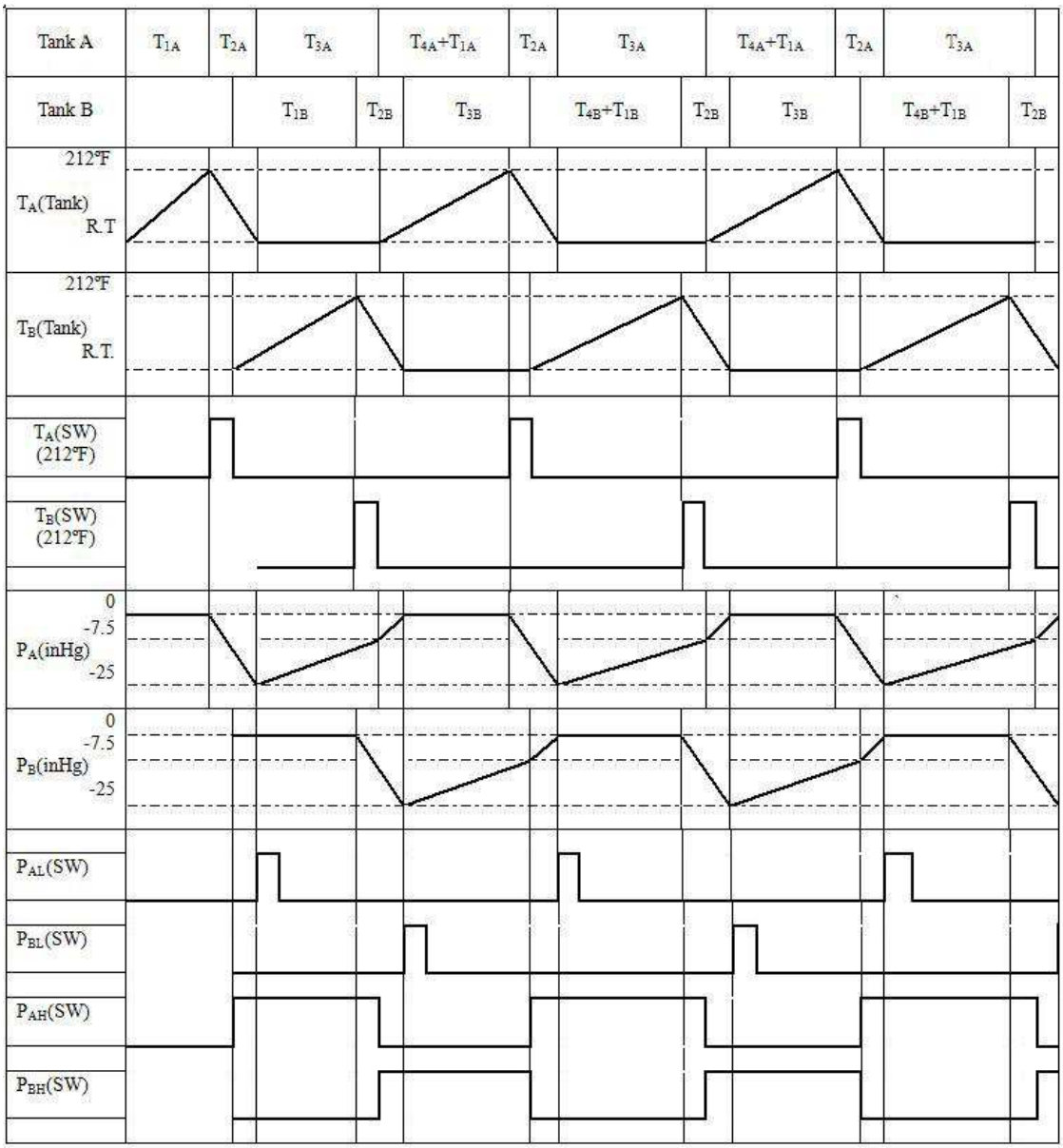

Figure 3.4 Process timing and signals from temperature and pressure switches in discontinuous operation case.

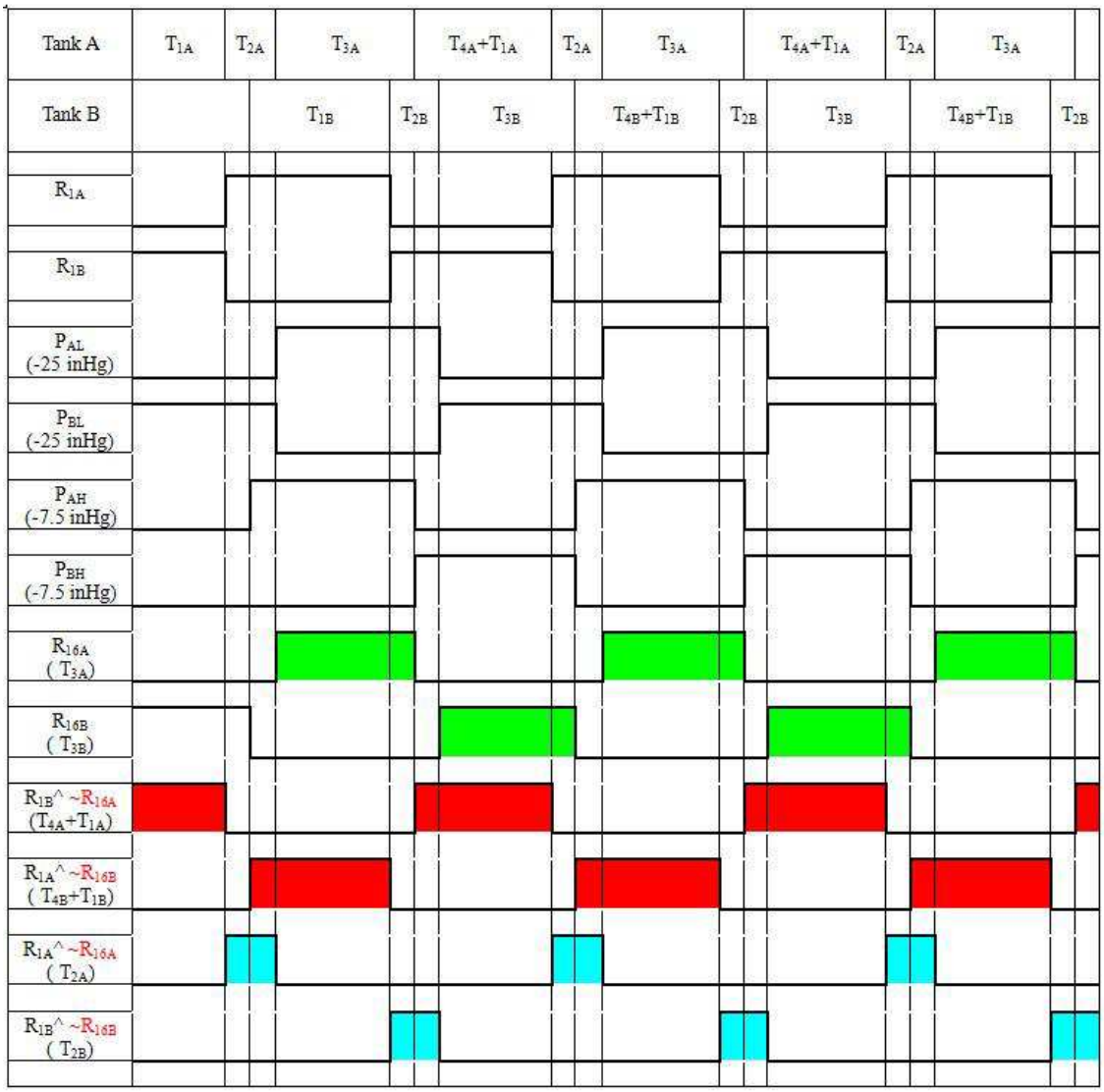

Figure 3.5 Process logic operations in discontinuous operation case.

3.3 Ladder Logic Diagrams for Process Control

The ladder logic has been designed for automatic control heating (Air Flush) and cooling (Depressurization) process of current thermal system. All other components used for implementing the control system, such as power supply, temperature and pressure switches, latching, timing and other relays, panel and indicators were specified during the development of the control logic. The control system is designed in a way so it can be operated in either automatic or manual modes. The ladder logic diagrams for the control panel and process control of heating and cooling cycle are shown in Appendix A.

3.4 Sustained Automatic Operation

For control design purpose, the vacuum generation process in each depressurization chamber is divided into four phases.

Steam Filling Phase (Duration T1): Currently this phase starts with tank at 1 atm to prevent water from entering the tank. Thus the duration is considered to be stable when the steam supply is stable. This phase starts with latching relay LR-T opens the steam supply valve V1A (or V1B). Vent valve 4 (NO) opens briefly then closes (through on-delay time relay TR4). The side heater (through relays RHA or RHB) and water outlet valve 8 (through repeat cycle relay TR8 with adjustable on/off time) are turned on. The vent valves 6 (NO) and 7 (NO) open for awhile then close through on-delay time relay TR6, adjustable between a selected range (and TR7, if need to be separately adjusted). The end of the phase is signaled by the temperature set point, e.g., 370~373 K with a temperature switch. Whenever the temperature in a tank reaches the set point, the steam supply is switched to the side of the other tank (through the latching relay LR-T), but the steam only enters the other tank (through valves 5A or 5B) when that tank is ready to

accept steam at the completion of its Transition Phase (T4, see below). Thus, there could be a waiting period between the opening of steam supply valve V1A (or V1B) and the actual steam filling through valve V5A (or V5B).

Cooling Phase (Duration T2): The duration is considered to be stable due to the similar initial condition and operation setting. Valves 5, 6, 7, and 8 are all closed. The side heater is turned off and the cooling water supply valve 9 (through relay R9A or R9B) is turned on. The end of the phase is signaled by the vacuum pressure set point ($P_g = P_{low}$) with a pressure switch PAL (or PBL), with the help of another latching relay LR-P.

Usage Phase (Duration T3): The duration is considered to be variable, depending on the flow rate of the air exchange (i.e. the usage rate). The repeat cycle relay TR8 is off, but the relay for valve 8 is on to close the valve. The relay for cooling water supply R9 is turned off. Valves 5, 6, and 7 remain closed. The end of the phase is signaled by another vacuum pressure set point ($P_g = P_{high}$) with another pressure switch PAH (or PBH) together with the latching relay LR-P, whichever comes first.

Transition Phase (Duration T4): Transition from vacuum use to vacuum generation. Currently this phase is needed to bring the tank pressure from Pa < 101.325 kPa (1 atm) to Pa = 101.325 kPa (1 atm). The duration is considered to be short. Since the end of phase T4 is the start of phase T1. This phase will be combined with phase T1 and implemented with a time delay in the start of the Phase T1. While the end of the phase can be signaled by another vacuum pressure set point, an adjustable time delay is used for now.

The states of the process are sum summarized as:

Phase T1: T ≈ ambient temperature → **370 K**; $P_g \approx 0$ Pa (Information not used).

Phase T2: $P_g = 0$ Pa → P_{low}; T = 370 K → ambient temperature (Information not

used).

Phase T3: $P_g = P_{low} \rightarrow P_{high}$, can exit the phase early if the use of the other fresh tank is preferred when the other tank is ready before the current tank is spend; T = ambient temperature → unspecified (Information not used).

Phase T4: $P_g = P_{high}$ (or lower) → 0 Pa; T ≈ ambient temperature (Information not used).

Since the transition from T4 to T1 is not detected by any means, the two phases are thus combined as:

Phase T4+ T1: T≈ ambient temperature → **370 K**; $P_g = P_{high}$ (or lower) → 0 Pa.

The following table shows the state of system components in each phase of the process (**RED** indicates the control relays should be energized).

Table 3.1 States of Components in the Process

	T4+T1	T2	T3
Valve 1 (NO)*	Open (R1 OFF)	Closed **(R1 ON)**	Closed **(R1 ON)**
Valve 4 (NO) **	Open→Closed (**TR4**→R4)	Closed **(R4 ON)**	Closed **(R4 ON)**
Valve 5 (NO) **	Closed→Open (**TR5**→R5)	Closed **(R5 ON)**	Closed **(R5 ON)**
Valves 6,7 (NO) **	Open→Closed (**TR6**→R6)	Closed **(R6 ON)**	Closed **(R6 ON)**
Valve 8 (NO) **	Open/Closed (**TR8**→R8)	Closed **(R8 ON)**	Closed **(R8 ON)**
Valve 9 (NC)	Closed (R9 OFF)	Open **(R9 ON)**	Closed (R9 OFF)
Valve 16 (NC)*	Closed (R16 OFF)	Closed (R16 OFF)	Open **(R16 ON)**
Side Heater (NO)	ON **(RH ON)**	OFF (RH OFF)	OFF (RH OFF)

To maintain the symmetrical arrangement of the twin-tank system, it is decided to use NO (Normally Open) for both valves 1A and 1B, and NC (Normally Closed) for both valves 16A and 16B. This approach helps to avoid change relay logic when no specific tank is designated as the starting tank. Proper initialization of the two latching relays LR-T and LR-P for their synchronized operation is implemented in the control logic.

Time delay for valves 4, 5, 6/7 and 8 are shown as follow.

Valve 4 (NO) – on delay, wait to close, for pipe to purge air.

Valve 5 (NO) – off delay, wait to open, for tank to reach 101.325 kPa (1 atm).

Valve 6/7 (NO) – on delay, wait to close, for tank to purge air.

Valve 8 (NO) – repeat cycle, on/off time.

The coordination of the two depressurization chambers (assuming depressurization chamber A is the starting tank) is worked as the following way.

At t=0 (the start of the operation), steam enters tank A and no action in tank B.

At t=T1 (the temperature in tank A reaches 370 K), steam supply is switched to the side of tank B. Tank A enters phase T2 and tank B enters phase T1. Tank B lags tank A by T1.

At t = T1+T2 (the pressure in tank A reached P_{low}), tank A enters phase T3. Since T1>T2, tank B is still in phase T1. In case that T1<T2 (not true in the current situation), tank B already entered phase T2 and the steam has switched back to the side A (but not entering tank A yet).

At t = T1+T2+T3 (the pressure in tank A comes back to P_{high} due to usage), tank A enters phase T4+T1. Vents in tank A opens for a preset time so it reaches 1 atm then closed. Steam enters tank A. Since T3>T1, tank B enters phase T3 before tank A finishes T3 and

the vacuum supply is witched to tank B. If there is no usage of vacuum, then a feedback is needed in the future to prevent too frequent switches between the two tanks. In case that T3<T1, tank B is not yet ready to supply vacuum, the operation becomes discontinuous.

At t = T1+T2+T3+ (T4+T1), tank A enters phase T2 and repeats step 2. Since T3>T4+T1, tank B is still in phase T3. Tank A should reach phase T3 again before tank finishes its phase T3. That is the obvious condition for continuous operation, T3≥ T4+T1+T2. While steam supply is switched from the side of tank A to the side of tank B, the steam will only enter the tank B after the tank B becomes ready to take the steam.

When the operation is continuous, the usage of vacuum (even though the amount may vary) is always less than the supply of vacuum, T3 will be stable. Thus, T3A=T4B+T1B+T2B, and T3B=T4A+T1A+T2A. If T3A<T4B+T1B+T2B and/or T3B=T4A+T1A+T2A, system could not reach the sustained operation. Control of steam supply based on usage of vacuum should be investigated if waste of vacuum becomes an issue.

Normal Operation:

1. Relay switch for Steam Heater R0: NO, Power ON → Heater ON This will be implemented outside the control loop, but a proper relay switch and indicator will be used on the main control panel.
2. Latching Relay LR-T (CO): switch power between sides A and B, latch and reset with temperature switches TA and TB; only one of the two outputs R1A and R1B is energized. Thus, one of the supply valves V1A (NO) and V1B (NO) is always open.

3. Vent Valve 4 (NO) Relay R4 is controlled through time-delay relay TR4 for "OFF for t4 then ON" so the valve can open for a delay of t4, then closed when control voltage is applied through R1A or R1B. The valve should remain closed (i.e. ON) during other periods.
4. Inlet Valve 5 (NO) Relay R5 is controlled through time-delay relay TR5 for "ON for t5 then OFF" so the valve is closed for a delay of t5, then becomes open when control voltage is applied during phase T4 and T1. The valve should remain closed (i.e. ON) during phase T2 and T3.
5. Vent Valves 6 and 7 (NO) Relay R6 and R7 are controlled through time-delay relay TR6 for "OFF for t6 then ON" so the valve is open for a delay of t6, then become closed when control voltage is applied during phase T4 and T1. The valve should remain closed (i.e., ON) during phase T2 and T3.
6. Condense Water Valve 8 Relay R8 is controlled through a repeat cycle relay, adjustable on/off time, ON when control voltage is applied during phase T4 and T1. The valve should remain closed (i.e. ON) during phase T2 and T3.
7. Cooling Water Valve 9 (NC) Relay R9: ON during phase T2, OFF during T3+T4+T1.
8. Side Heater Relay RH (NO): ON during phase T4+T1, OFF during T2+T3
9. Latching Relay LR-P (CO): identify the entrance to Phase T3 for either side A and side B, latch and reset with pressure switches PAL, and PBL; used together with PAH or PBH to mark the Phase T3. Valve 16 (NC) Relay R16 is ON only during T3.

The experiment is conducted for sustained automatic operation of the test chamber for 70 SCFH air flow rate (20 SCFH fresh air + 50 SCFH of re-circulation of air from test chamber) for 3 hrs. With frequent automatic opening and closing of condensate drain valve, the heating time of the system was considerably reduced. The sustained supply of vacuum under automatic operation in the current system is shown in Figure 3.6.

The manually controlled operation cycle consists of four phases: heating time, depressurization time, wait time and operation time. While in automatic sustain operation, the wait time is removed by switching automatically the connection of test chamber to the newly prepared depressurization chamber, even though the vacuum in the current depressurization chamber may not be completely used up (i.e., its pressure has not reached to its limiting value, P_{high}).

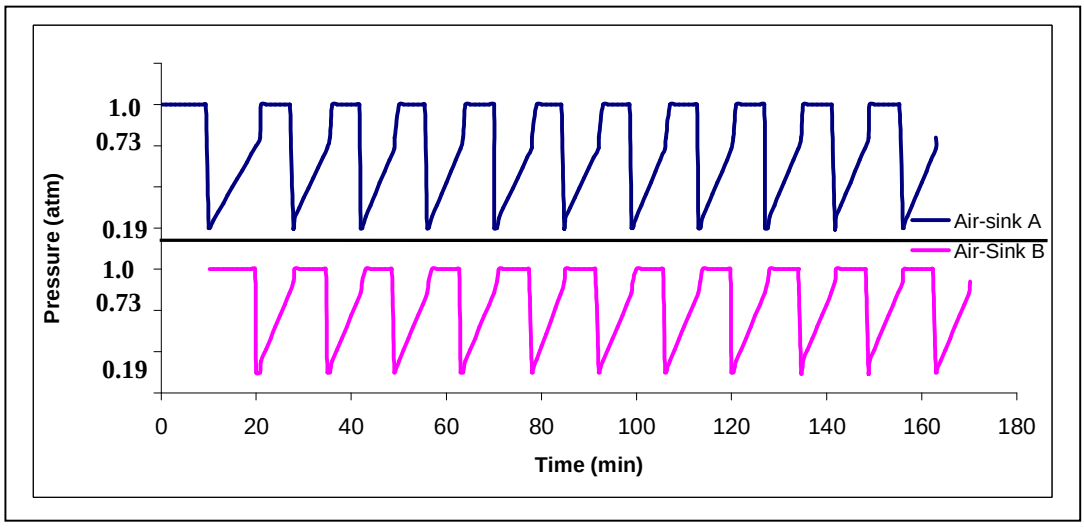

Figure 3.6 Sustain automatic controlled operation with pressure variation in depressurization chambers A & B.

CHAPTER 4

ANALYSIS OF OPERATION PHASES

Chapter 3 discussed the implementation of the control system for the laboratory-scaled experimental setup. During this implementation, many process parameters, such as timing of the open and closure of the certain valves, were adjusted based on the knowledge obtained through previous experiments using manual operation. Since most of the parameters are essential in developing an accurate, safe and quick response control system, a further analysis of the relationship between those parameters and the states of the process, such as real-time temperatures and pressures of the chambers, is conducted in this chapter for the three main phases of the operation: the steam filling phase, cooling phase and usage phase.

4.1 Analysis of Steam Filling Phase

The steam filling phase describes the flushing process of air from adiabatic depressurization chamber with the saturated steam. The purpose of this process is to fill the chamber full with steam as the preparation for the subsequent depressurization in the cooling phase.

This phase starts with the chamber full of air at an atmosphere pressure (e.g., 101.325 kPa) at room temperature (about 293 K) in the current experimental setup. Then, the saturated steam at 101.325 kPa (at 373 K) from the steam generator is supplied through a control valve to the chamber. The steam enters the chamber and mixes with air already in the chamber. Some of the mixture leaves the chamber through another valve at the exit. Temperature and pressure of this mixture inside the chamber change as more steam filled

into the chamber. And finally, the air inside the depressurization chamber will be replaced with steam vapor after sufficient time of flushing.

The assumptions for the modeling of the process are stated below.

(1) Air and steam are both treated as ideal gas, same as in earlier chapters.

(2) The condensation of steam during the flushing process is ignored. This assumption is justified with the analysis in Section 4.1.1.

(3) A perfect mixing and instant thermal equilibrium between air and steam is assumed. This assumption is made only to simplify the initial analysis. The content of vapor should be higher near the steam inlet, while the content of air near the chamber exit should be higher than the average. The analysis presented in this section can be modified when more accurate mix model becomes available.

4.1.1 Treatment of Condensate During Steam Filling

During the rapid expansion of steam, a condensation process will take place shortly after the state path crosses the vapor-saturation line. This causes the dry steam to form a two-phase mixture of saturated vapor and fine liquid droplets known as a wet steam. The liquid mass fraction (also known as wetness factor) is used to describe the level of condensation in the steam.

The state equation of wet steam can be written as follows by using wet steam virial coefficient [24],

$$P = \rho_v RT(1 + B\rho_v + C{\rho_v}^2) \tag{4.1}$$

where B, and C are the second and the third virial coefficients given by the following empirical functions:

$$B = a_1(1 + \frac{\tau}{\alpha})^{-1} + a_2 e^{\tau}(1 - e^{-\tau})^{\frac{5}{2}} + a_3\tau \tag{4.2}$$

where B is given in m^3/kg, $\tau = \frac{1500}{T}$ with T given in Kelvin, $\alpha = 10000.0$, $a_1 = 0.0015$, $a_2 = -0.000942$, and $a_3 = -0.0004882$.

$$C = a(\tau - \tau_0)e^{-\alpha\tau} + b \tag{4.3}$$

Where C is given in m^6/kg^2, $\tau = \frac{T}{647.286}$ with T given in Kelvin, $\tau_0 = 0.0015$, $\alpha = 11.16$, $a = 1.772$, and $b = 1.5 \times 10^{-6}$.

The two empirical functions that define the virial coefficients B and C cover the temperature range from 273K to 1073K.

Compare with the state equation without considering the condensation, that is B = 0 and C = 0 as dry steam, the pressure differences at selected temperatures are shown in Table 4.1 and Figure 4.1.

These results illustrate that in the current working range of temperature from 323K to 383K, the values of the virial coefficients B and C are small and thus the difference in the computed pressure between “dry steam” and “wet steam” is quiet small. The liquid mass fraction is therefore assumed to be zero and steam maintains its dry state after

entering the tank. The influence of the condensate during the steam flushing is ignored in the subsequent analysis.

Table 4.1 Comparison of Dry Steam and Wet Steam

T (k)	323	333	343	353	363	373	383
p_{wet} (Pa)	12288.06	19822.87	30932.18	46898.09	69208.57	99704.57	140457
p_{dry} (Pa)	12350	19940	31190	47390	70140	101400	143300
$(p_{wet} - p_{dry})/ p_{wet}$	0.50%	0.64%	0.83%	1.04%	1.33%	1.67%	1.98%

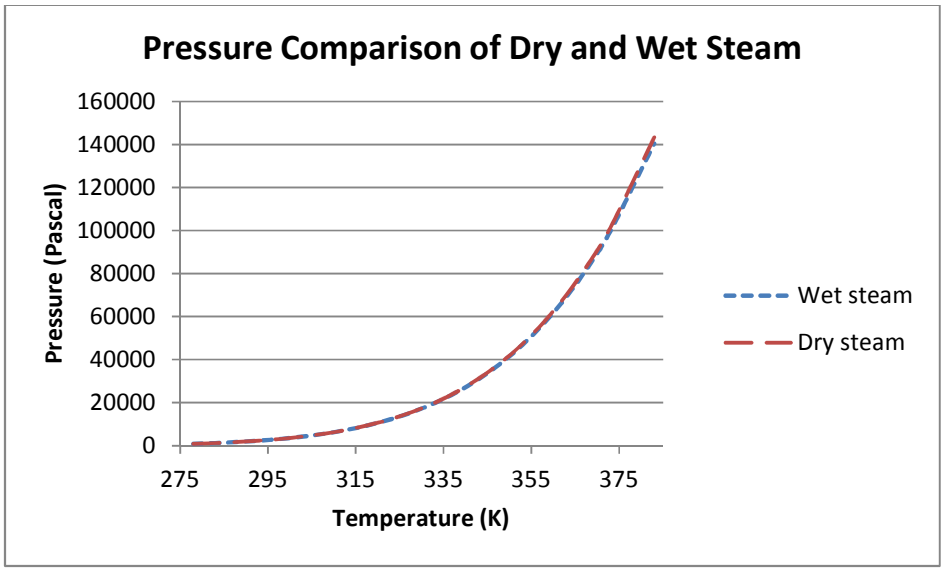

Figure 4.1 Pressure comparison of dry and wet steam.

4.1.2 Modeling of the Steam Filling Process

In the steam filling phase, the saturated steam is provided to fill the depressurization chamber with steam vapor. A schematic figure is show in Figure 4.2. The key factors in this process are the mass of the steam at inlet (m_i), chamber pressure (p_1) and temperature (T), the mass of vapor (m_v) and air (m_a) inside the depressurization chamber and the mass of exit mixture (m_e).

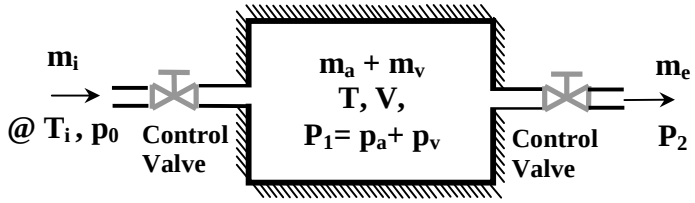

Figure 4.2 A schematic figure of steam filling process.

The steam inlet flow rate mainly depends on the specific control valve used in the process and the pressure drop between the valve inlet pressure and outlet pressure. For the low pressure drop as in this experiment, the steam inlet flow rate for the control valves can be calculated with Equation 4.4 [25],

$$Q_s = 1.06\sqrt{d_0 p_0}\, c_g \sin\left[\frac{3417}{c_1}\sqrt{\frac{p_0 - p_1}{p_0}}\right] deg \tag{4.4}$$

where,

C_1: C_g/C_v

C_g: Gas sizing coefficient

C_v: Liquid sizing coefficient

d_0: Density of steam or vapor at inlet, lbs/ft^3

p_0: Valve inlet pressure, psia

p_1: Valve outlet pressure, psia

Q_s: Steam or Vapor mass flow rate, lb/hr

The outlet flow of the depressurization chamber is a mixture of steam and air. The mass or molar ratio of the steam and air in the mixture changes when more steam fills into the depressurization chamber and less air remains inside the depressurization chamber. The outlet flow rate is also controlled by the control valve. Since, the outlet gas is no longer pure steam, a new equation is adopted here. For universal gas, not only confined to steam, the valve flow rate could be expressed in Equation 4.5 [25].

$$Q = \sqrt{\frac{520}{GT}}\ p_1\, c_g \sin\left[\frac{3417}{c_1}\sqrt{\frac{p_1 - p_2}{p_1}}\right] deg \tag{4.5}$$

Similarly, the parameters are listed below.

G: Gas specific gravity

T: Absolute temperature of gas at inlet, degree Rankine

Q: Gas volume flow rate, ft^3/hr

p_1: Valve inlet pressure, psia

p_2: Valve outlet pressure, psia

C_1: C_g/C_v

C_g: Gas sizing coefficient

C_v: Liquid sizing coefficient

To describe the process of the steam filling, several more equations are required. Equations could be built based on the mass conservation law, energy balance law and state equation for perfect gas.

For mass conservation of the air,

$$\frac{dm_a}{dt} = 0 - \frac{dm_e}{dt} \cdot \frac{m_a}{m_a + m_v} \tag{4.6}$$

For mass conservation of the steam,

$$\frac{dm_v}{dt} = \frac{dm_i}{dt} - \frac{dm_e}{dt} \cdot \frac{m_v}{m_a + m_v} \tag{4.7}$$

Combining Equation 4.6 with Equation 4.7, there is the mass conservation of the system,

$$\frac{m_a}{dt} + \frac{dm_v}{dt} = \frac{dm_i}{dt} - \frac{dm_e}{dt} \tag{4.8}$$

An average mass ratio, γ, of vapor to the total mass inside the depressurization chamber is defined in Equation 4.9. It is also the mass ratio of vapor in the exit mixture

under the perfect mixing assumption.

$$\gamma = \frac{m_v}{m_a + m_v} \tag{4.9}$$

So, the Equation 4.6 and Equation 4.7 can be expressed as,

$$\frac{dm_a}{dt} = 0 - \frac{dm_e}{dt} \cdot (1 - \gamma) \tag{4.10}$$

$$\frac{dm_v}{dt} = \frac{dm_i}{dt} - \frac{dm_e}{dt} \cdot \gamma \tag{4.11}$$

where,

$\frac{dm_i}{dt}$ = Steam inlet flow rate

$\frac{dm_a}{dt}$ = Mass rate of air inside the depressurization chamber

$\frac{dm_v}{dt}$ = Mass rate of vapor inside the depressurization chamber

$\frac{dm_e}{dt}$ = Mixture flow rate exit (air + vapor)

From an energy balance point of view, Equation 4.12 is written below,

$$\frac{d(m_a u_a + m_v u_v)}{dt} + m_T c_T \frac{dT}{dt} = \frac{dm_i}{dt} h_i - \frac{dm_e}{dt} h_e \tag{4.12}$$

Since,

$$\frac{d(m_a u_a)}{dt} = u_a \frac{dm_a}{dt} + m_a \frac{du_a}{dt} = u_a \frac{dm_a}{dt} + m_a c_{va} \frac{dT}{dt} \tag{4.13}$$

$$\frac{d(m_v u_v)}{dt} = u_v \frac{dm_v}{dt} + m_v \frac{du_v}{dt} = u_v \frac{dm_v}{dt} + m_v c_{vv} \frac{dT}{dt} \tag{4.14}$$

Hence,

$$u_a \frac{dm_a}{dt} + u_v \frac{dm_v}{dt} + (m_a c_{va} + m_v c_{vv} + m_T c_T) \frac{dT}{dt} = \frac{dm_i}{dt} h_i - \frac{dm_e}{dt} h_e \tag{4.15}$$

where,

h_i: Specific enthalpy of inlet steam (determined by T_i and p_i)

u_a: Specific internal energy of air inside the depressurization chamber

h_a: Specific enthalpy of air inside the depressurization chamber

u_v: Specific internal energy of vapor inside the depressurization chamber

h_v: Specific enthalpy of vapor inside the depressurization chamber

h_e: Specific enthalpy of gaseous mixture (air + vapor)

m_T: Mass of the steel tank

c_T: Specific heat of steel = 510 J $kg^{-1}K^{-1}$

c_{pa}: Constant-pressure specific heat of air

c_{va}: Constant-volume specific heat of air

c_{pv}: Constant-pressure specific heat of steam

c_{vv}: Constant- volume specific heat of steam

R_a: Specific gas constant of air = 287 J $kg^{-1}K^{-1}$

R_v: Specific gas constant of steam = 461.5 J $kg^{-1}K^{-1}$

$$u_a = c_{va}T$$

$$h_a = c_{pa}T$$

$$u_v = u_{ref} + c_{vv}(T - T_{ref})$$

$$h_v = h_{ref} + c_{pv}(T - T_{ref})$$

$$h_e = \frac{m_v h_v + m_a h_a}{m_v + m_a}$$

$u_{ref} = 2375000\,\frac{J}{kg}$; $h_{ref} = 2500000\,\frac{J}{kg}$; $T_{ref} = 273K$.

Constant-pressure specific heats and constant-volume specific heats of air and steam (c_{pa}, c_{pv}, c_{va} and c_{vv}) change with the temperature. The relationships are listed below [26].

$$c_{pa} = 1.05 - 0.365 \times \left(\frac{T}{1000}\right) + 0.85 \times \left(\frac{T}{1000}\right)^2 - 0.39 \times \left(\frac{T}{1000}\right)^3$$

$$c_{va} = c_{pa} - R_a$$

$$c_{pv} = 1.79 - 0.107 \times \left(\frac{T}{1000}\right) + 0.586 \times \left(\frac{T}{1000}\right)^2 - 0.20 \times \left(\frac{T}{1000}\right)^3$$

$$c_{vv} = c_{pv} - R_v$$

By applying the perfect gas state equation to both air and steam, we can get the Equation 4.16 to Equation 4.19.

$$m_v = \frac{p_v V}{R_v T} \tag{4.16}$$

That's,

$$\frac{dm_v}{dt} = -\frac{m_v}{T}\frac{dT}{dt} + \frac{m_v}{p_v}\frac{dp_v}{dt} \tag{4.17}$$

Gas state equation of air inside the chamber

$$m_a = \frac{p_a V}{R_a T} \tag{4.18}$$

And there is a relationship $p_1 = p_a + p_v$,

Then,

$$\frac{dm_a}{dt} = -\frac{m_a}{T}\frac{dT}{dt} - \frac{V}{R_a T}\frac{dp_v}{dt} + \frac{V}{R_a T}\frac{dp_1}{dt} \tag{4.19}$$

Now, there are seven unknowns, p_1, m_a, m_v, m_e, T, p_v, m_i, and seven independent equations from above analysis. The unknowns could be found by solving these equations.

In our current experimental case, the control valves are pneumatic actuated ball valve from Assured Automation 101 series. For these specific valves in 1 inch size, $C_1 = 22$ [25], $C_v = 117$ [27], $C_g = C_1 C_v = 2574$.

For the inlet flow, if the provided saturated steam is 102.00 kPa (14.847 psi), the density and pressure are $d_0 = 0.755\ kg/m^3 (= 0.047133\ lbs/ft^3)$, $p_0 = 102.00$ kPa (14.847psia). The initial pressure of the depressurization chamber is set as $p_1(0) = 101.325$ kPa (14.7 psia).

The units of Equation 4.4 can be changed into international system (SI) unit.

$$\frac{dm_i}{dt} = 1.26 \times 10^{-4} Q_s = 1.3356 \times 10^{-4} \times \sqrt{d_0 p_0}\, c_g \sin\left[\frac{3417}{c_1}\sqrt{\frac{p_0 - p_1}{p_0}}\right] deg \tag{4.20}$$

For the outlet flow, the valve inlet pressure is the tank pressure p_1, the valve outlet pressure is the outside air pressure p_2, where $p_2 = 101.325$ kPa (14.7 $psia$). As the air and steam mixture, the outlet gas specific gravity G can be expressed in the following format.

$$G = \frac{m_v}{m_a + m_v} G_v + \frac{m_a}{m_a + m_v} G_a \tag{4.21}$$

where, $G_v = 0.6218$, water vapor specific gravity and $G_a = 1.0$, air specific gravity.

Change Equation 4.5 into SI unit, then,

$$\frac{dm_e}{dt} = 7.87 \times 10^{-6} \frac{m_a + m_v}{V} \sqrt{\frac{520}{G \times \frac{9}{5} T}} \; p_1 \, c_g \sin\left[\frac{3417}{c_1} \sqrt{\frac{p_1 - p_2}{p_1}}\right] deg \tag{4.22}$$

From the above analysis, the pressure change, temperature change and mass change of steam filling phase can be calculated. The volume of the depressurization chamber, a 30 gallon steel chamber is set as V=0.11149 m^3 in the calculation. The results for 60 seconds of the vapor pressure and temperature change inside the depressurization chamber in this phase are shown in Figure 4.3. Figure 4.4 illuminates the mass change inside the chamber for 60 seconds.

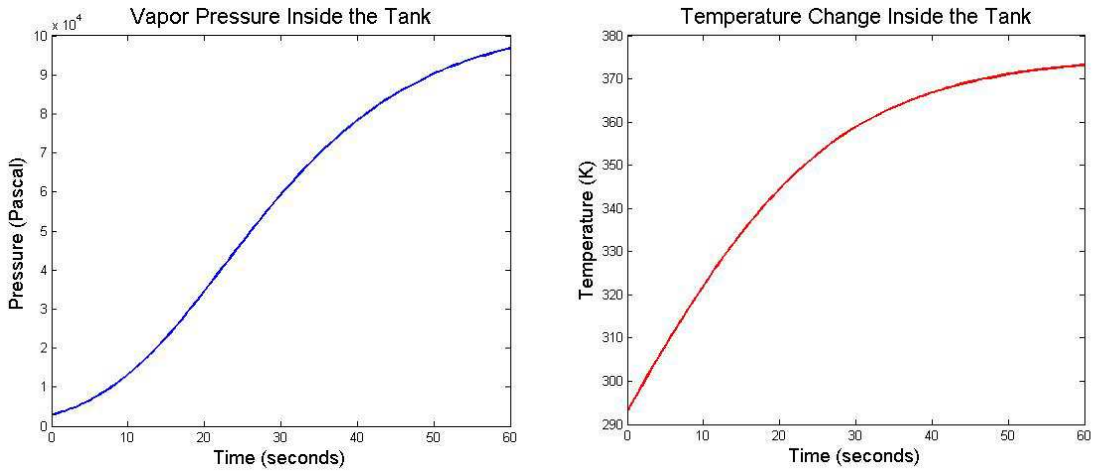

Figure 4.3 Vapor pressure change and temperature change during steam filling phase.

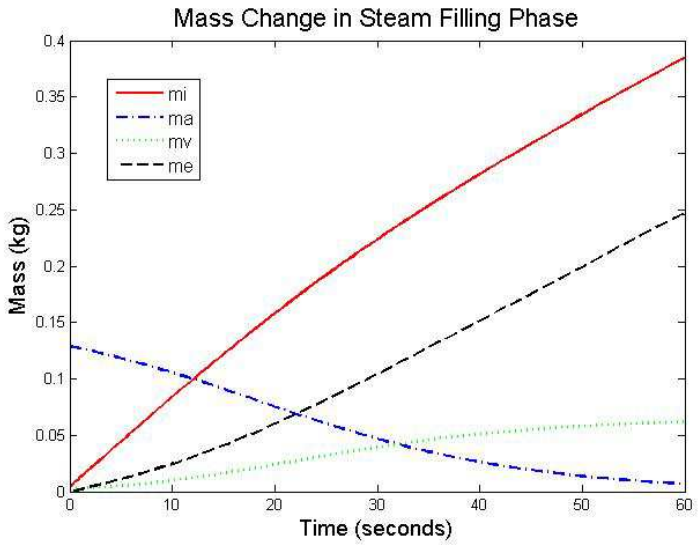

Figure 4.4 Mass change during steam filling phase.

4.2 Analysis of Cooling Phase

The primary objectives of this theoretical modeling for the cooling phase are to explore and quantify the mechanistic effects of thermal non-equilibrium and various key parameters on the transient characteristic of condensation-controlled depressurization. In this section, a

thermodynamics model which provides the characteristics of the depressurization process during the cooling phase is developed. And the results are presented and discussed.

4.2.1 Modeling of the Cooling Phase

In order to provide the quantitative analysis of depressurization process without neglecting the most dominating mechanisms (such as condensation on cooling coil, chamber depressurization, and heat storage effect of chamber wall), a simple thermodynamics model is developed. The schematic diagram for this process is shown in Figure 4.5.

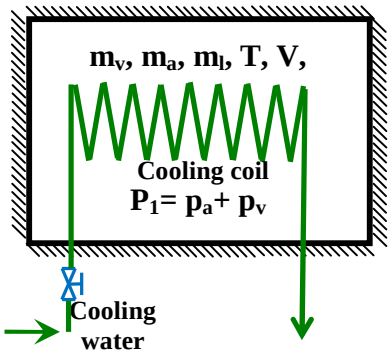

Figure 4.5 A schematic figure of depressurization process.

The most important assumptions in this model include:

(1) Instant thermal equilibrium between the steam (including condensate) and coil tube (including water inside the coil);

(2) Very large thermal capacity of chamber wall with heat convection to steam and thermal radiation between chamber wall to cooling coil;

(3) A small amount of non-condensable (NC) gases (air in this case) inside the chamber.

The total mass and energy of vapor, condensates and NC gas (air) in the chamber is conserved during the depressurization, which can be expressed as,

$$\frac{d}{dt}(m_v + m_l + m_a) = 0 \tag{4.23}$$

Based on the species conservation (without reaction), the mass of the air inside the chamber remains constant and hence,

$$\frac{dm_a}{dt} = 0 \tag{4.24}$$

From the first law of thermodynamics, the energy balance yields:

$$\begin{aligned}&(m_p c_p + m_{ch} c_{ch} + m_v c_{vv} + m_l c_l + m_a c_{va})\frac{dT}{dt} \\ &= L\frac{dm_l}{dt} - \dot{m}_c c_c (T - T_c)\end{aligned} \tag{4.25}$$

The vapor partial pressure is related to the vapor temperature by the Clapeyron-Clausius equation:

$$\frac{dp_v}{dT} = \frac{p_v L}{R_v T^2} \tag{4.26}$$

The total pressure of the system is the sum of the partial pressures of vapor and air, according to the Dalton's law:

$$p_1 = p_a + p_v \tag{4.27}$$

Based on the ideal gas law, the mass of steam and air inside the system can be written (by ignoring the volume of condense), respectively, as:

$$m_v = \frac{p_v V}{R_v T} \tag{4.28}$$

$$m_a = \frac{p_a V}{R_a T} \tag{4.29}$$

In summary, the simplified model consists of seven independent equations, Equations 4.23 — 4.29 and seven variables (m_v, m_l, m_a, p_v, p_a, p_1, T), and hence the problem is closured.

4.2.2 Results and Discussion

To solve the aforementioned coupled governing equations of the theoretical model, appropriate inlet boundary conditions need to be identified. The temperature and pressure of the steam inside the confined chamber was at 373 K and atmospheric pressure respectively. The mass flow rate and temperature of the coolant at the inlet to the chamber was 0.35 kg/s and 278 K respectively. Due to lack of experimental data on the percentage of air (non-condensable gases) present into the chamber, the percentage of impurity was set

to 0 %. That is, $T(0) = 373\ K$, $P_1(0) = 101.325\ kPa$, $m_v(0) = 0.06687\ kg$, $m_l(0) = 0\ kg$, $dm_c/dt = 0.35\ kg/s$, and $T_c = 278\ K$.

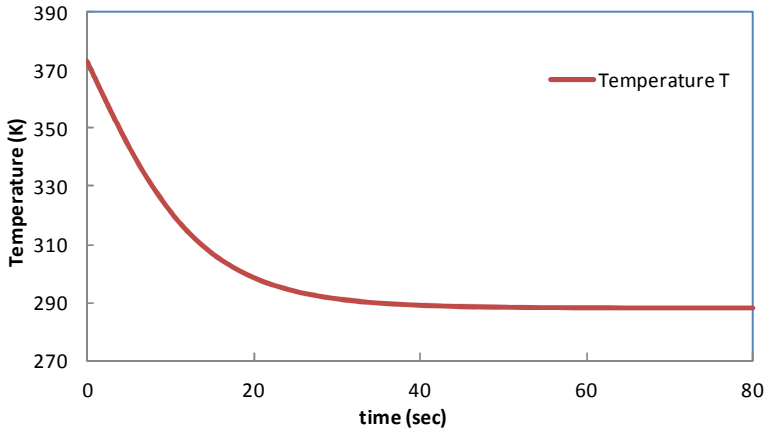

Figure 4.6 Temperature predictions in the cooling phase.

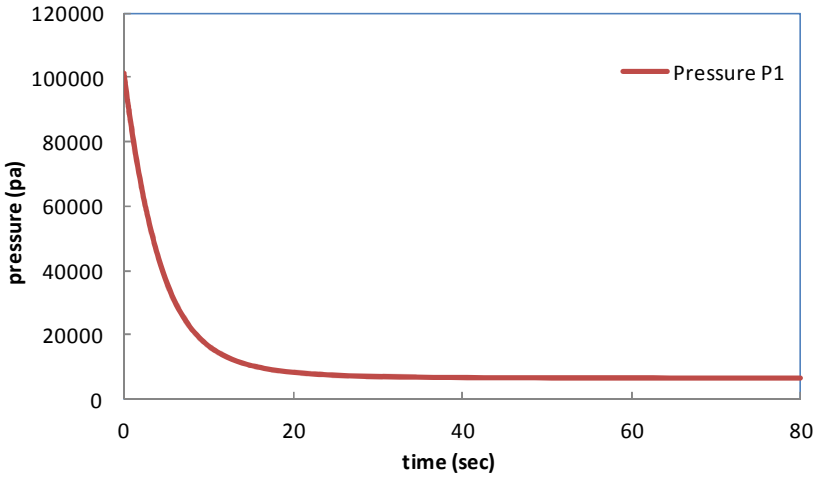

Figure 4.7 Pressure predictions in the cooling phase.

The predictions of this theoretical model are shown in Figures 4.6 and 4.7. The temperature drops fast around the first 20 seconds. And in a similar pattern, chamber

pressure decreases evidently during the first 10 seconds to about 20 kPa. These results reasonably predict the depressurization process.

It should be pointed out that, for the model predictions in Figure 4.6 and Figure 4.7, the effect of non-condensable gases (air) on the depressurization characteristics is ignored. The non-condensable gases are always present into the system. Even a small amount of such gases may have significant influence on the pressure of the system, especially on the final chamber pressure after the cooling. Figure 4.8 shows the effect of non-condensable gases impurity inside the chamber on the depressurization characteristics. The final steady-state pressure of the system at the end of the depressurization process has been significantly affected by the amount of non-condensable gases inside the system. Results show that as the initial molar percentage of non-condensable gas increases inside the system, the final steady-state pressure of the system also increases. By comparing with the asymptotic value from the measurements in Figure 4.7, the initial molar percentage of air in the system is approximated about 10%, as shown in Figure 4.8.

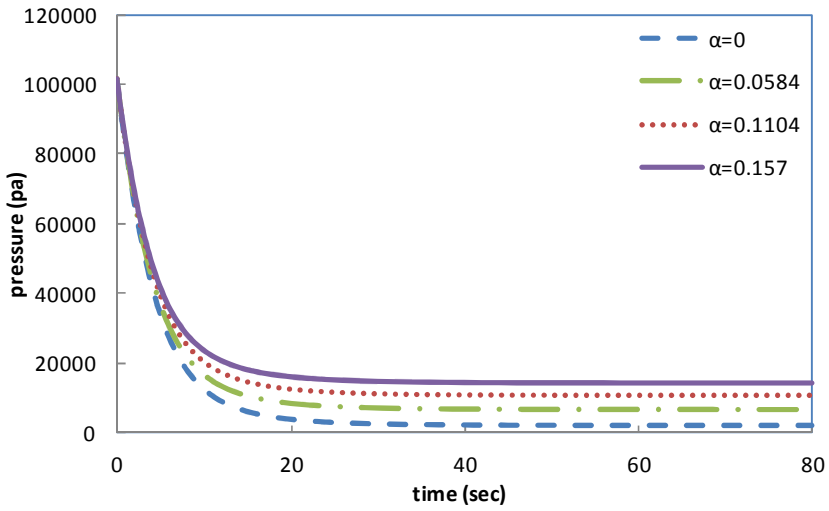

Figure 4.8 Effect of NC gas on pressure.

A preliminary assessment on the parametric effects of depressurization characteristics can be obtained using the simplified model. The influence of non-uniformity and thermal non-equilibrium can be minimized if the comparison between two similar cases of the same system is based on the relative ratio of depressurization time. In other words, even though the modeling predictions may be considerably different from the actual results, the trend and the percentage reduction in depressurization time with the percentage increase in coolant flow rate can be close to that of actual case.

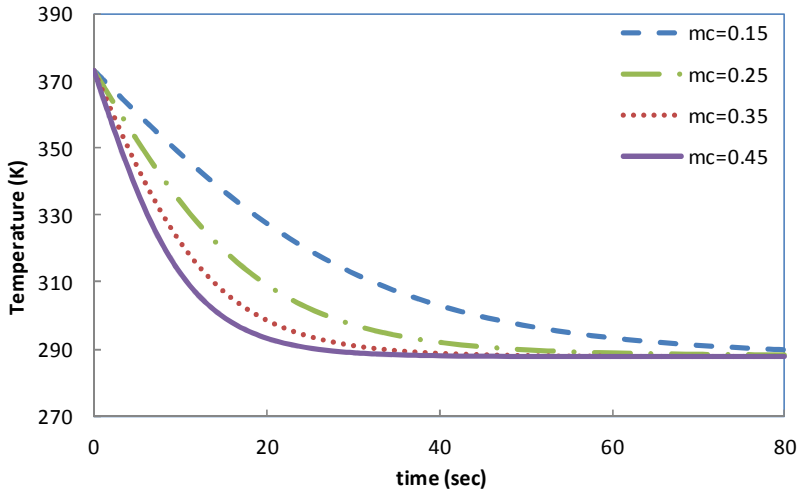

Figure 4.9 Effect of coolant flow rate on chamber temperature.

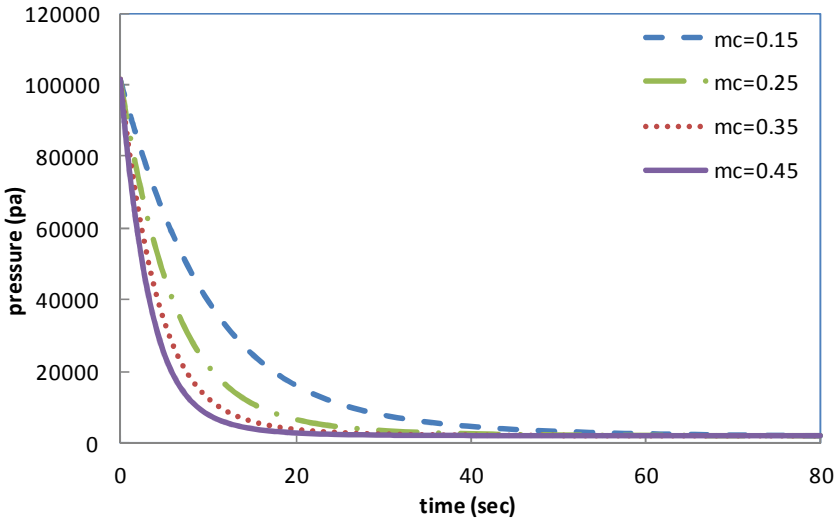

Figure 4.10 Effect of coolant flow rate on chamber pressure.

Figures 4.9 and 4.10 illustrate the predicted effect of coolant flow rate on time-dependent system pressure and temperature during the depressurization process. As expected, the increase in the coolant flow rate can significantly shorten the depressurization time. For example, increasing the coolant mass flow rate from 0.15 kg/s to 0.45 kg/s (increased by 300%), the depressurization time (to reach the steady state pressure) is reduced from 60 sec to 24 sec (60% reduction) as shown in Figure 4.10. In addition, the depressurization rate is much faster at the initial stage with increasing of coolant mass flow rate.

4.3 Analysis of Usage Phase

While the generated vacuum can be used in various applications, the analysis of the usage phase in this study is focused on the test chamber for the altitude effect study as an example. The test chamber is worked as a confined usage environment. In the test chamber, pressure, humidity, temperature, purity of the air, are all important parameters to be monitored and controlled. In this section, models are built to analysis this usage process.

4.3.1 Chamber Pressure Change

First of all, pressure is the key parameter under the current study. To study the pressure change in test chamber and depressurization chambers, a thermodynamic model of the test chamber and its interaction with outside air and the depressurization chamber is developed. Figure 4.11 illustrates the interface of the test chamber with its working environment.

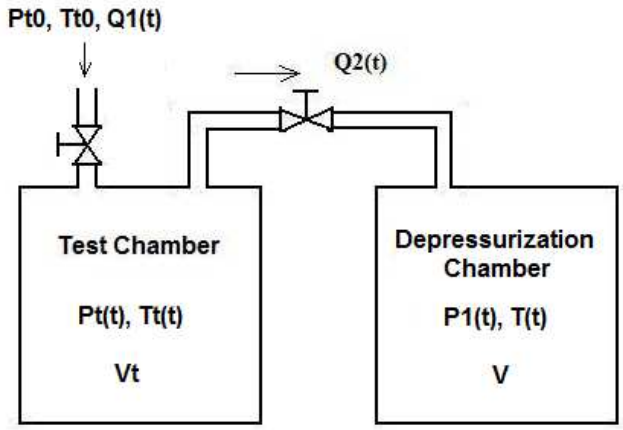

Figure 4.11 Simplified schematic of vacuum interface.

The notations used in the analysis are as follows:

p_{t0}: Source air pressure

p_t : Pressure in test chamber

p_1 : Pressure in depressurization chamber

ρ_0 : Density of source air

ρ_1 : Density of air in test chamber

ρ_2 : Density of air in depressurization chamber

V_t : Volume of test chamber

V : Volume of depressurization chamber

M : Volume ratio V_1 / V_2

Q_1 : Air flow rate into test chamber

Q_2 : Air flow rate into depressurization chamber

T_{t0} : Temperature of source air

T_t : Temperature in test chamber

T : Temperature in depressurization chamber

t : Time

Since the working range of the operational pressure is much less than the critical pressure of the air and the working range of the operational temperature is more than twice of the critical temperature of the air, ideal gas law can be applied to the air in the system (inside both chambers as well as ambient air). Thus,

$$\frac{p_i}{\rho_i T_i} = R = \frac{R_u}{M_a} \qquad (i = 0,1,2) \tag{4.30}$$

where, the universal gas constant R_u =8.3145 J/(K mol), the molar mass of air M_a = 28.97×10^{-3} kg/mol, and the specific gas constant R =286.9 J/(kg K).

By applying mass conservation in both the test chamber and the depressurization chamber, Equation 4.31 and Equation 4.32 can be obtained.

$$\frac{d\rho_1}{dt}V_1 = \rho_0 Q_1 - \rho_1 Q_2 \tag{4.31}$$

$$\frac{d\rho_2}{dt}V = \rho_1 Q_2 \tag{4.32}$$

By using Equation 4.30, the two other equations could be got,

$$\frac{d}{dt}\left(\frac{p_t}{T_t}\right) = R\frac{d\rho_1}{dt} \tag{4.33}$$

$$\frac{d}{dt}\left(\frac{p_1}{T}\right) = R\frac{d\rho_2}{dt} \tag{4.34}$$

From Equations 4.30, 4.31 and 4.33, a new equation is developed as shown below.

$$\frac{d}{dt}\left(\frac{p_t}{T_t}\right) = \frac{p_{t0}Q_1}{V_1 T_{t0}} - \frac{p_t Q_2}{V_1 T_t} \tag{4.35}$$

In the current operation setting, $T_{t0} = T_t$ (both at room temperature). Thus, Equation 4.35 becomes,

$$\frac{dp_t}{dt} = \frac{1}{V_1}(p_{t0}Q_1 - p_tQ_2) = \frac{1}{MV}(p_{t0}Q_1 - p_tQ_2) \tag{4.36}$$

From Equation 4.32 and Equation 4.34,

$$\frac{d}{dt}\left(\frac{p_1}{T}\right) = \frac{1}{T}\left(\frac{dp_1}{dt} - \frac{p_1}{T}\frac{dT}{dt}\right) = \frac{p_t}{T_tV}Q_2 \tag{4.37}$$

During the usage phase, air is drawn from the test chamber into the depressurization chamber which causes change in temperature T_t and pressure p_1 in depressurization chamber.

Let m_{20} be the air mass inside the depressurization chamber at the start of the usage phase and m_{1t} be the air mass drawn from test chamber into depressurization chamber during the use. The total mass of the mixed air in depressurization chamber is their sum:

$$m_2 = m_{1t} + m_{20} \tag{4.38}$$

Thus,

$$m_{1t} = m_2 - m_{20} = \rho_2V_2 - \rho_{20}V_2 \tag{4.39}$$

From the energy balance consideration in the depressurization chamber

$$m_{1t}h_{a1} = m_2 h_{a2} - m_{20}h_{a20} \tag{4.40}$$

where, $h_{a1} = c_{pa}T_t$, $h_{a2} = c_{pa}T$ and $h_{a20} = c_{pa}T_0$. Then,

$$m_2 T = m_{1t}T_t + m_{20}T_0 \tag{4.41}$$

From Equation 4.39 and Equation 4.40, we can get,

$$\rho_2 V_2 T = (\rho_2 V - \rho_{20} V)T_t + \rho_{20} V T_0 \tag{4.42}$$

By using equations of state of gas, Equation 4.42 can be written as

$$p_1 \frac{M_a V}{R} = p_1 \frac{M_a V T_t}{RT} + p_{10} \frac{M_a V}{R}\left(1 - \frac{T_t}{T_0}\right)$$

or,

$$p_1 = p_1 \frac{T_t}{T} + p_{10}\left(1 - \frac{T_t}{T}\right) \tag{4.43}$$

This leads to a relation between the pressure and the temperature in the depressurization chamber as,

$$p_1 = p_1 \frac{T}{T_0}\left(\frac{T_0 - T_t}{T - T_t}\right) \tag{4.44}$$

or

$$T = \frac{p_1 T_0 T_t}{(p_1 - p_{10})T_0 + p_{10} T_t} \tag{4.45}$$

With T_t =293K (room temperature), Equation 4.45 establishes the relationship between state parameters T and p_1 when they deviate from the initial values. Figure 4.12 illustrates this relation with the initial values of T_0 =353K, and $p_{10} = 2.34 \times 10^4$ Pa (0.2313 atm). It shows that pressure increases while the temperature decreases when cooler air drawn into the chamber.

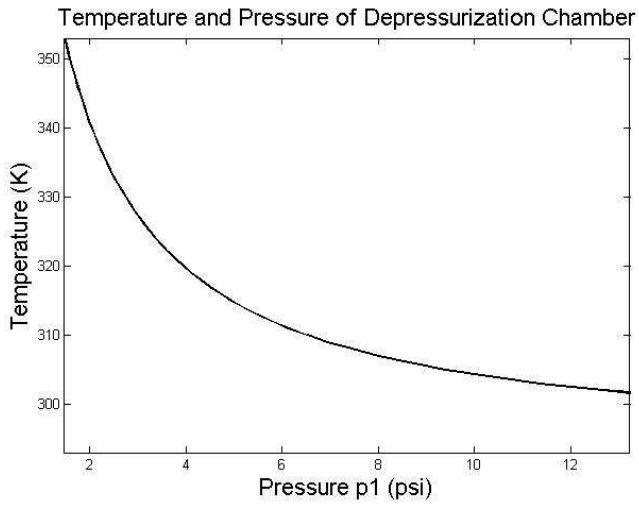

Figure 4.12 Relation between temperature and pressure in depressurization chamber at usage phase.

The above discussion does not consider the effect of copper tube inside the chamber and the steel tank body. Including this factor into the model, Equation 4.40 should be written as:

$$m_{1t}h_{a1} = m_2 h_{a2} - m_{20}h_{a20} + M_{steel}c_{steel} \cdot \Delta T \tag{4.46}$$

where M_{steel} is the mass of tank, c_{steel} is specific heat capacity of steel. Compare with the steel tank, the mass of copper tube inside the chamber is quite small. So, the heat effect of the copper tube is neglected. Since $\Delta T = T - T_0$, $h_{a1} = c_{pa}T_t$, $h_{a2} = c_{pa}T$, $h_{a20} = c_{pa}T_0$ and $m_{1t} = m_2 - m_{20}$, Equation 4.46 above can be rewritten as,

$$c_{pa}(m_2 - m_{20})(T - T_t) = (c_{pa}m_{20} + c_{steel}M_{steel})(T_0 - T) \tag{4.47}$$

In the experimental system, m_2 is less than 0.1kg, and M_{steel} is around 12.5 kg. M_{steel} is much larger than m_{20} and $(m_2 - m_{20})$. With $c_{pa} = 1.005kJ/kgK$ and $c_{steel} = 0.510kJ/kgK$, $(T_0 - T)$, the change of T, is very small. The relation between T and p_1 is shown in Figure 4.13 according to Equation 4.47.

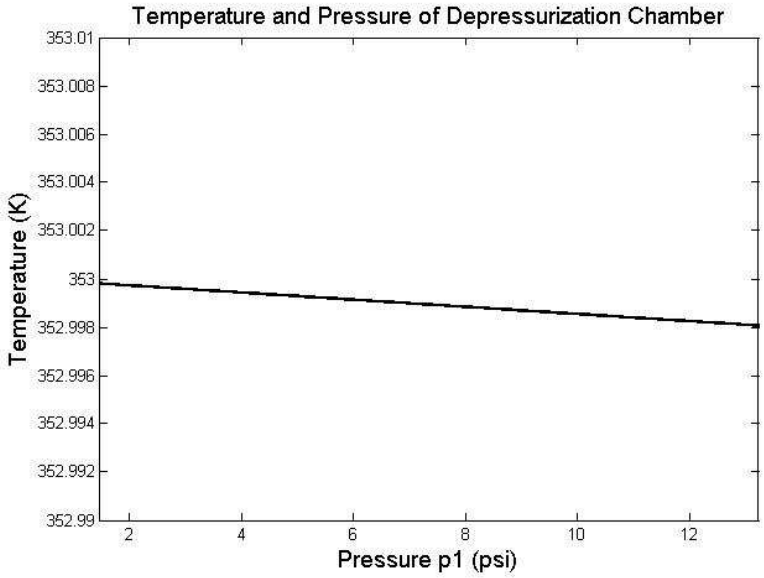

Figure 4.13 Relation between temperature and pressure considering the heat of tank.

Temperature in depressurization chamber T varies little from the initial temperature T_0 when pressure increases. This phenomenon has been confirmed in the actual experiments.

To simplify the future calculation, T is treated as a constant. With this simplification, Equation 4.37 becomes,

$$\frac{dp_1}{dt} = \frac{p_t T}{V T_t} Q_2 \tag{4.48}$$

The amount of air, $m_{1t}(t)$, drawn from the test chamber to the depressurization chamber, in order to change the pressure of exchange chamber from its initial state p_{10} to certain pressure $p_0(t)$ can now be estimated as,

$$m_{1t} = m_2 - m_{20} = \frac{V}{R_u}\left(\frac{p_1(t)}{T} - \frac{p_{10}}{T_0}\right) = \frac{\Delta p_1 \cdot V}{R_u T} \tag{4.49}$$

The air-drawing capacity is affected by the pressure change Δp_1 and volume V of the depressurization chamber. This will be used to estimate the duration that the depressurization chamber can be sustained for maintaining the desired pressure in the test chamber. We define this duration time as vacuum holding time T_H. From Equation 4.36 and Equation 4.48 we can see that $p_1(t)$ is related to p_t, Q_1 and Q_2. Thus, it is necessary to understand the relationships between p_t and Q_1, Q_2.

4.3.2 Inlet and Outlet Flow Rate of Test Chamber

To control the flow rate of vacuum interface between depressurization chamber and test chamber, vacuum regulator is needed. Vacuum regulators are widely used in process plants. They maintain a constant vacuum at the regulator inlet with a higher vacuum connected to the outlet. During the operation, a vacuum regulator remains closed until a vacuum decrease (a rise in absolute pressure) exceeds the spring setting and opens the valve disk. Opening the valve plug permits a downstream vacuum of lower absolute pressure than the controlled vacuum to restore the upstream vacuum to its original setting.

The constant pressure desired is represented by the set-point. It is determined by the initial compression of the regulator spring. By adjusting the initial spring compression you change the spring loading force, thus the pressure at the regulator inlet side (p_1). This establishes the set-point.

Figure 4.14 is a typical performance curve of vacuum regulators from the manufacturer [28]. The regulated pressure p_1 drops below set-point as flow increases. The droop is the amount of deviation from set-point at a given flow, expressed as a percentage of set-point. This “droop” curve is important to a user because it indicates regulating capacity

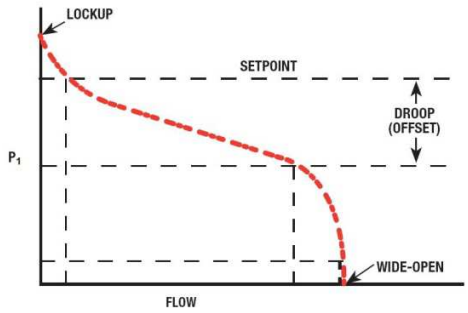

Figure 4.14 Typical performance curve of the vacuum regulator [28].

Capacities published by regulator manufacturers are given for different amount of droop. Although changing the orifice size can increase capacity, a regulator can pass only so much flow for a given orifice size and inlet pressure. Once the regulator is wide-open, reducing p_1 does not result in higher flow. This area of the flow curve identifies critical flow.

In the experimental system, a type D-51 vacuum regulator [29] is used. It is designed for use in systems where it is desired to maintain, automatically, a lower vacuum at the valve inlet than prevails at the source on the valve outlet, which is what we need. The valve inlet is connected to the test chamber of the system in which the lower vacuum is to be held; valve outlet is connected to the depressurization chambers. Spring is adjusted for correct vacuum on inlet side, which is around 6" Hg vacuum. Outlet side is subjected to

depressurization chambers at the initial vacuum of 25" Hg. Any change in controlled vacuum produces valve movement to correct for that change, thus maintaining inlet vacuum within very narrow limits.

The capacity curve for type D-51 vacuum regulator [30] is obtained from the supplier and the graph is shown in Appendix B. To make the information useable in the analysis, the original plot is digitized and then converted into a polynomial curve through regression. A curve is fitted for a pressure at 7.42×10^4 Pa (8" Hg vacuum or 0.7326atm), which is close to the pressure used in experiment, in the form 4th order polynomial as shown in Figure 4.15.

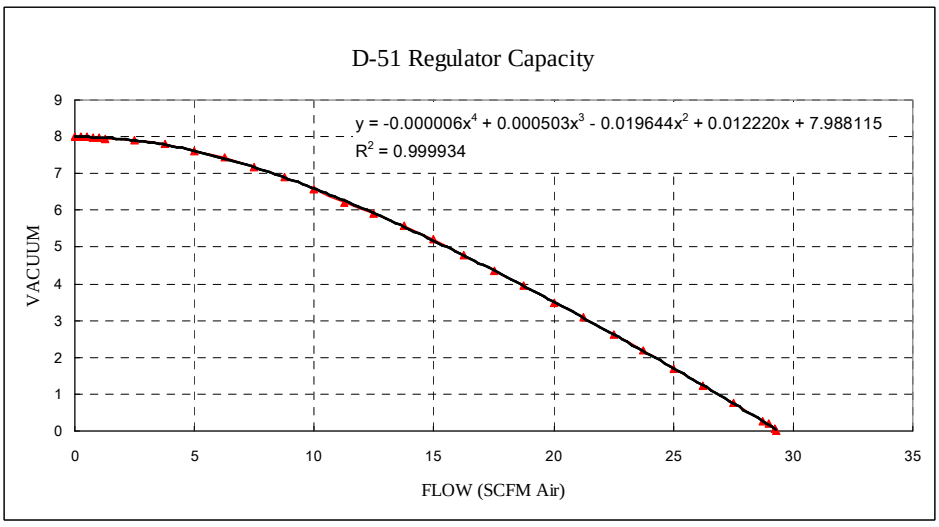

Figure 4.15 Capacity curve 1 for D51 at 8" Hg vacuum.

The fitting equation is shown in Equation 4.50 and the R-squared value of the fitting is $R^2 = 0.999934$.

$$p_t = -0.000006Q_2^{\,4} + 0.000503Q_2^{\,3} - 0.019644Q_2^{\,2} + 0.012220Q_2 + 7.988115 \qquad (4.50)$$

The same digitized capacity curve has also been fitted to express flow rate Q_2 in terms of pressure p_t, whose unit used in the fitting has been changed from inch of Hg (" Hg) vacuum to psia. The fitted curve is shown in Figure 4.16 and the corresponding polynomial equation is,

$$Q_2 = -0.3293\,p_t^{\,4} + 17.218\,p_t^{\,3} - 336.94\,p_t^{\,2} + 2930.7\,p_t - 9559.4 \qquad (4.51)$$

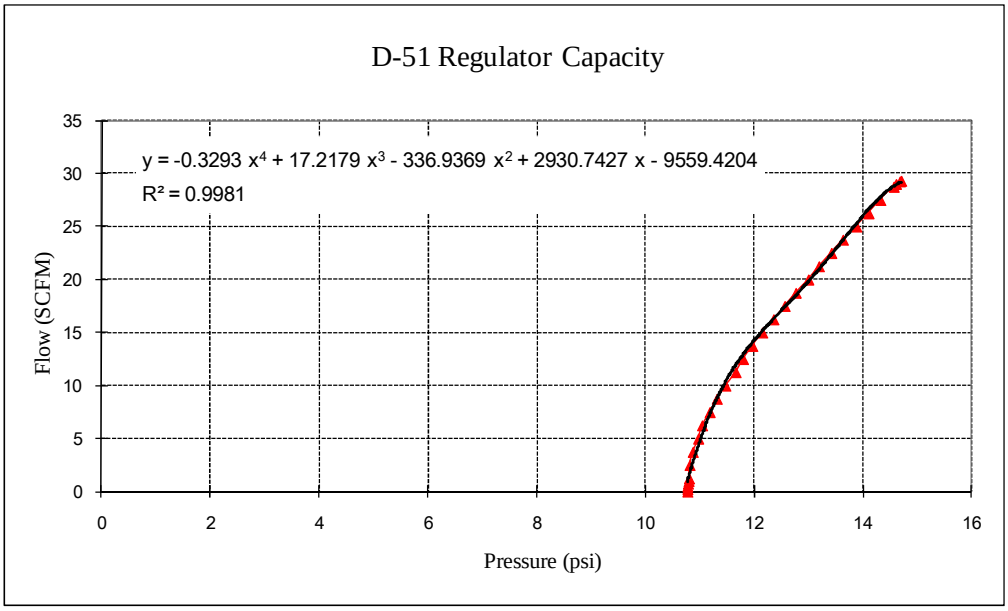

Figure 4.16 Capacity curve 2 for D51 at 8" Hg vacuum.

The same approach can be used to obtain relationship between Q_2 and p_t at different pressure settings in test chamber. Equation 4.52 is the result of the fitting with the setting pressure in test chamber at 8.10×10^4 Pa (6" Hg vacuum or 0.7995 atm). The fitted

curve is shown in Figure 4.17. This pressure setting is actually closer to the experimental setting than the previous case.

$$Q_2 = -0.8717\,p_t^{\,4} + 46.971\,p_t^{\,3} - 948.37\,p_t^{\,2} + 8510.2\,p_t - 28642 \tag{4.52}$$

And $R^2 = 0.9974$.

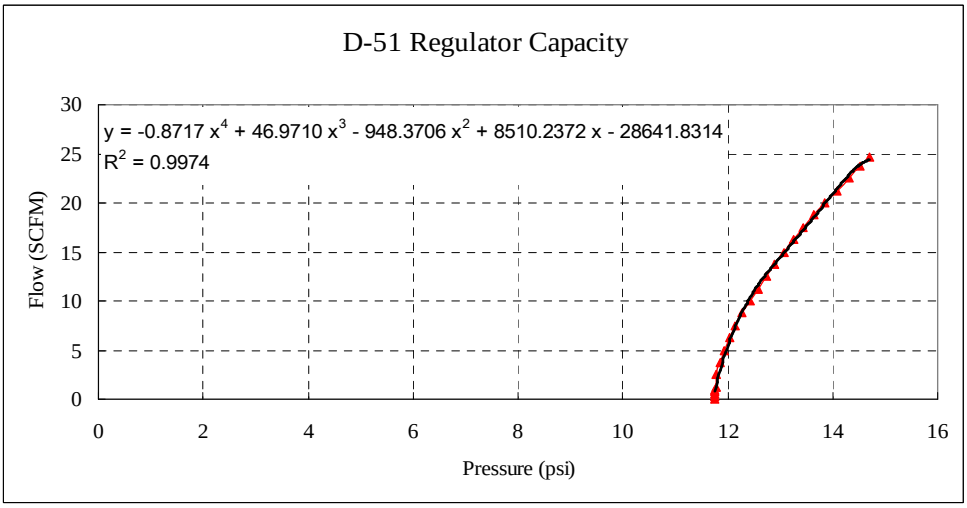

Figure 4.17 Capacity curve for D51 at 6" Hg vacuum.

The flow rate Q_1 of test chamber is the inlet air flow into the test chamber. In the experimental system, its air supply consists of both fresh air from the outside and re-circulated filtered air. Let $Q_{outside}$ be the flow rate of outside air and Q_{rec} be the flow rate of re-circulated air. The portion of the air from recirculation can expressed as,

$$Q_{rec} = \beta \cdot Q_{supply} \quad (0 < \beta < 1) \tag{4.53}$$

Thus, the portion of the air from outside can be expressed as

$$Q_{outside} = (1-\beta)Q_{supply} \tag{4.54}$$

Let the chamber volume be $V_{chamber}$ and the chamber air exchange rate be λ. Then we have the relationship,

$$V_{chamber} = \lambda \cdot Q_{\text{supply}} = \frac{\lambda}{1-\beta} Q_{outside} \tag{4.55}$$

The vacuum interface focus on the inlet flow rate Q_1, outlet flow rate Q_2, test chamber pressure p_t, the volume of test chamber V_1 and the volume of depressurization chamber V in the current analysis, as shown in Figure 4.5. Here, Q_1 in the experimental system is equivalent to $Q_{outside}$. If half of the air is from recirculation, then $\beta = 0.5$. The following equation can be written,

$$2Q_1\lambda = V_1 \tag{4.56}$$

In the experimental system, the volume of the test chamber is set as V_1=3.9372 ft^3 and the air exchange rate is set to λ= 3 minutes. Thus $Q_1 = 0.6562$ ft^3/min.

4.3.3 Results and Discussion

In analytical solution, several parameters, boundary and initial conditions are set as follows.

1. Dimension of the test chamber and depressurization chamber

The dimensions of test chamber and depressurization chamber are the same. The diameter and height of the chamber are $D = 18.25$ in, $H = 27.5$ in. So, the volume of the chamber is

$$\pi(D/2)^2 \cdot H = 4.1630 \text{ ft}^3 = 0.11788 \text{ m}^3$$

Considering the volume of cooling tubes inside the tanks and thickness of the wall, the actual volume of test chamber and depressurization chamber is considered as:

$$V_1 = V = 3.9372 \text{ ft}^3 = 0.11149 \text{ m}^3$$

2. Boundary conditions

Source air pressure $p_{t0} = 1.01 \times 10^5$ Pa (14.7 psi)

Source air temperature $T_{t0} = 293$ K=528 R

Temperature in test chamber $T_t = 293$ K

Temperature in depressurization chamber $T = 353$ K

3. Initial conditions at time t=0

Pressure in test chamber $p_t(0) = 1.01 \times 10^5$ Pa (14.7 psi)

Pressure in depressurization chamber $p_1(0) = 1.01 \times 10^4$ Pa (1.47 psi)

Regulator flow rate $Q_1(0) = 0$ SCFM

Regulator flow rate $Q_2(0) = 29.3$ SCFM at regulator setting 8" Hg vacuum

$Q_2(0) = 24.7$ SCFM at regulator setting 6" Hg vacuum

Using the above operation parameters and initial conditions, the four independent Equation 4.36, Equations 4.48, 4.51 and 4.56 can be used to solve for the four unknowns: p_t, p_1, Q_1 and Q_2. Runge Kutta numerical method [31] is used to solve these differential

equations. Calculation for the specific case, a test chamber at $V_1 = 0.11149m^3$, is conducted. The results of pressure change and air flow rate are shown in Figure 4.18.

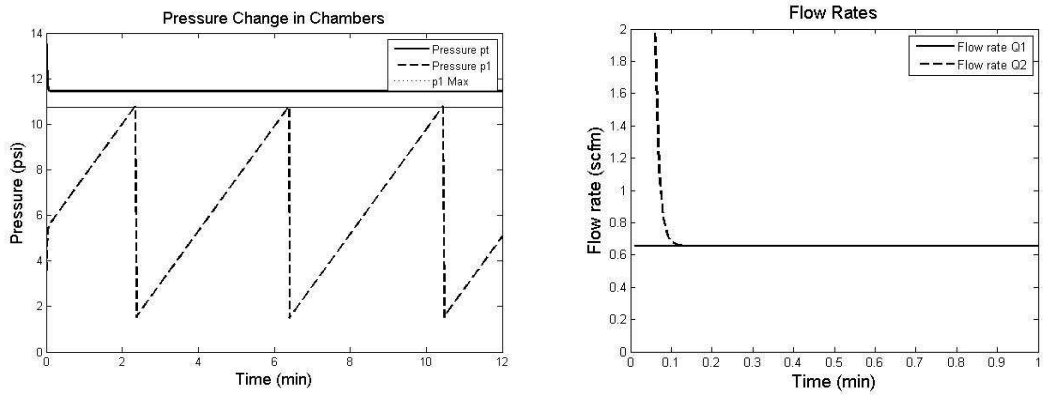

Figure 4.18 Pressures and flow rates vs. time in the usage phase.

The above results are based on the setting of the D-51 vacuum regulator to regulate at 6" Hg vacuum. Thus Equation 4.52 is used in the calculation. Different settings of the vacuum regulator can affect the pressure variation inside the test chamber and the vacuum holding capacity of depressurization chamber. A comparison to another setting, where the D-51 vacuum regulator is set to regulate at 8" Hg vacuum, is summarized in Table 4.2. Figure 4.19 shows the pressure differences of both the test chamber and the depressurization chamber in two cases.

Table 4.2 Comparison between Two Different D-51 Settings

V_1:V_2 Ratio M	Flow rate $Q_1 = Q_2$ (CF/Min)	D-51 Regulator setting	Pressure p_t (psi)	*Holding time T_H (min)
1	0.6562	6" Hg	11.4519	4.05
		8" Hg	10.7757	4.30

* Holding time is recorded once $p_1(T_H)$ reaches 7.42×10^4 Pa (10.76 psi=0.73 atm) when the system works continuously (without the initial effect).

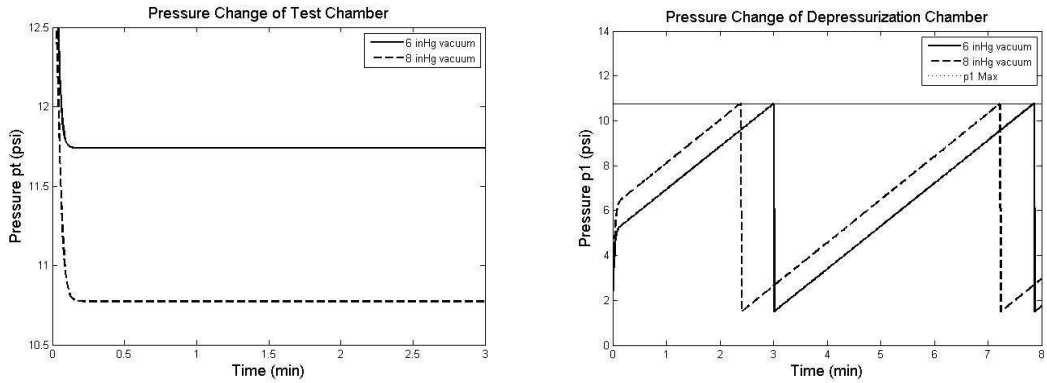

Figure 4.19 p_t, p_1 at different D-51 regulator settings.

From the above comparison, it could be found that in each single case, the higher vacuum setting by D-51 vacuum regulator, the lower absolute pressure in test chamber maintained, and the longer vacuum holding time for depressurization chamber persisted. As the flow rate increases, the differences between two settings reduced both in pressure in test chamber p_t and holding time T_H. That's because when the flow rate rises above 10 ft^3/min, the limit of regulator capacity itself couldn't make the pressure close enough to the original setting, and regulator works in a out of droop region. That's what needs to be avoided in the experiment.

4.3.4 Continuous Operation Requirements

The vacuum holding time T_H, as defined in Section 4.3.1, is the time period from the start of using the depressurization chamber to the point that the pressure in the depressurization chamber reaches its maximum design value $p_1\_\max = 7.42\times10^4$ Pa (10.76 psi), at which the depressurization chamber's ability to draw air from the test chamber is greatly diminished.

To ensure the sustained operation of the entire system with two depressurization chambers, the vacuum holding time T_H for one depressurization chamber must be longer than the time that needed to prepare the vacuum status of the other depressurization chamber. This preparation time is now referred to as vacuum generating time, T_G. The sustained operation thus requires $T_H > T_G$.

As illuminated in Chapter 3, the system process could be divided into four phases: steam filling phase (duration T1), cooling phase (duration T2), usage phase (duration T3) and transition phase (duration T4). Here, vacuum holding time T_H describes the usage phase, and vacuum generating time T_G describes the remaining there phases. Thus T_H = T3 and T_G = T4 + T1 + T2.

The modeling of steam filling phase (duration T1) was discussed in Section 4.1. The cooling phase (duration T2) was discussed in Section 4.2. During the transition phase (duration T4), the valves are open to the outside the air to let the pressure of the depressurization chamber changes from around the test chamber hypobaric setting pressure to the atmosphere pressure. In the current system, this transition is needed because the feeding water used to generate the steam is under the atmospheric pressure. If the chamber

pressure is lower than the atmospheric pressure, the water might be sucked into the depressurization chamber when the steam supply valve V1 is open. T4 is short as around 2 to 3 seconds based on the experiment results. This procedure is actually a loss of the hypobaric environment. For the future system improvement, a new design is under consideration which takes this hypobaric environment as an advantage to accelerate the steam filling.

At the current experimental setup, the timing for each phase is summarized in Table 4.3. It can be seen that $T_H > T_G$. The continuous operation of the system can be achieved.

Table 4.3 Timing of Four Phases of Current Experimental Setup

	Vacuum Generating Time T_G			Vacuum Holding Time T_H
	Transition Phase (T4)	Steam Filling Phase (T1)	Cooling Phase (T2)	Usage Phase (T3)
Time (seconds)	3	59	10	243

CHAPTER 5

DESIGN OF SYSTEMS FOR GENERAL APPLICATIONS

The analysis and results discussed in the previous chapters are based on an existing experimental system. The knowledge gained through this study can be extended to other practical applications of vacuum environment, where the volume of the hypobaric chamber can be much larger and the usage pattern of the vacuum can be quite different from this existing experiment system. The depressurization chambers must be properly designed so that the resulted vacuum holding time and the vacuum generating time can ensure the system's continuous operation.

In order to design the vacuum generation systems to satisfy the demand in different applications, several methods have been considered to produce more vacuum in less time. One approach is to use steam at higher pressure to shorten the filling time. Another approach is to eliminate the transition phase in the operation. The third approach is to select a good volume ratio between the depressurization chamber and hypobaric chamber to achieve more efficient coordination between the vacuum generation and usage. All these methods can be combined to form a better system structure for achieving continuous and high efficiency operation of the system. These issues are discussed in the following three sections. A general industry application guideline is presented in the last section.

5.1 Parametric Effects on Steam Supply

Currently, the steam is generated by a 10.5 kW electric heater. For other industry application design, a large power of boiler can be used to provide sufficient steam at faster flow rate. If the steam is supplied as the industry byproduct, saturated steam at higher pressure could be provided.

The effects of steam inlet pressures on the filling phase could be studied by using the theoretic model of steam filling phase, as discussed in Section 4.1. Although the modeling predictions may be different from the actual experimental results, the trend and the percentage reduction in steam filling time with the percentage increase in inlet steam pressure can be close to that of actual case.

Figure 5.1 and Figure 5.2 are the vapor pressure and temperature change inside the chamber at different saturated steam inlet pressure, 1.05 atm, 1.15 atm and 1.30 atm respectively. Figure 5.3 is the comparison of mass ratio of vapor and air inside the depressurization chamber, defined by Equation 4.9, at three different steam inlet pressures.

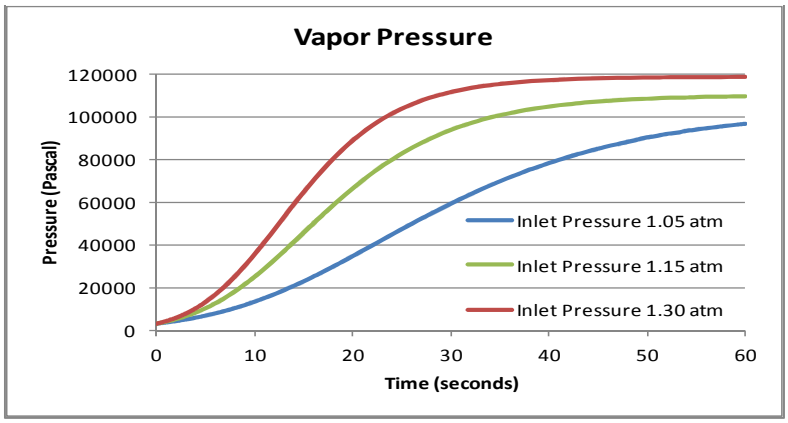

Figure 5.1 Effect of different steam inlet pressures on vapor pressure inside the depressurization chamber.

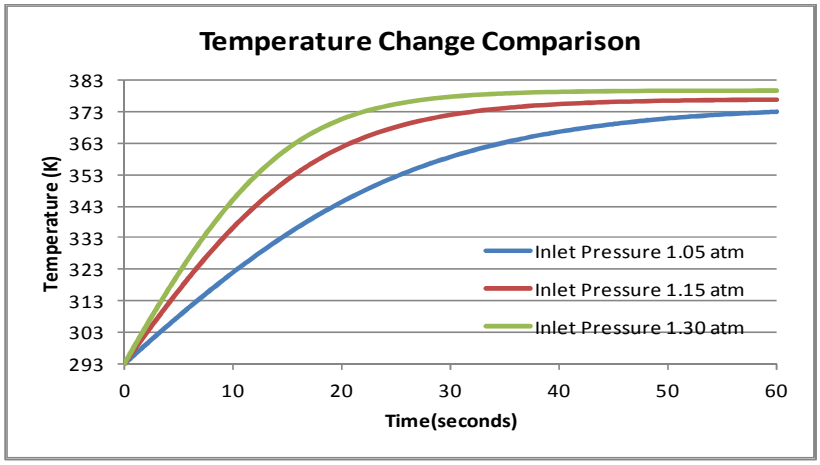

Figure 5.2 Effect of different steam inlet pressures on temperature change inside the depressurization chamber.

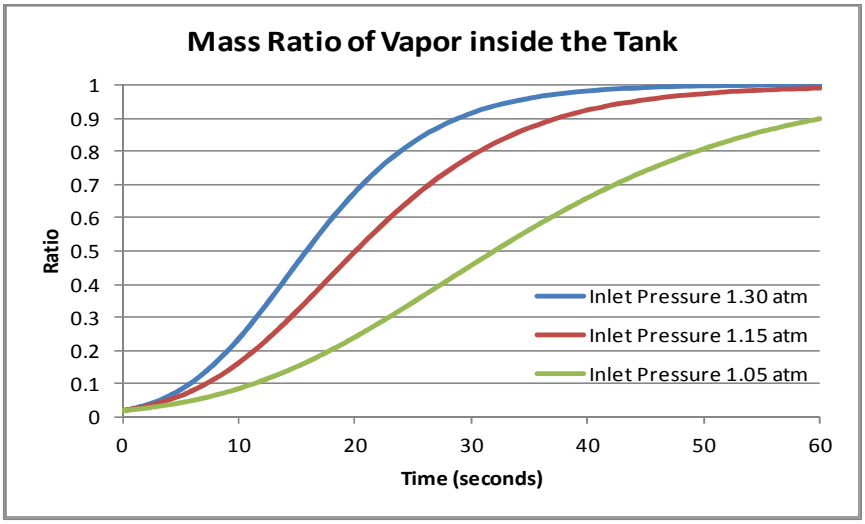

Figure 5.3 Effect of different steam inlet pressures on mass ratio of vapor inside the depressurization.

From the above three figures, it is clear that increase the inlet steam pressure will reduce the steam filling time. As shown in Figure 5.3, with the increase of inlet steam pressure by 10% and 25%, the time for mass ratio of vapor to the total gas mass inside the depressurization chamber to reach 90% reduces from 60 seconds to about 40 seconds and 30 seconds. Hence, increasing the pressure of supplied steam can be considered in the

future system design.

5.2 Effect of the Depressurization Chamber Volume

Both the volume of the test chamber and depressurization chamber are the same in the current experimental system. Since this is not a requirement, different volumes could be used in the future design. This volume ratio will certainly affect the relationship between the vacuum holding time and the vacuum generating time.

5.2.1 The Influence of the Volume to Vacuum Holding Time

First of all, the influence of the volume raise of the chambers to the vacuum holding time is discussed. Section 4.3 discussed the modeling of the vacuum usage. From Equations 4.36, 4.48, 4.51 and 4.56, the two relationships, $p_t = f(t, M, V, p_{t0}, \lambda)$ and $p_1 = f(t, M, V_2, p_{t0}, \lambda)$, could be obtained. Since source air pressure p_{u0} and air exchange time period λ are set as constants, p_{t0} = 101325 pa, λ = 3 minutes, they can be expressed as, $p_t = f(t, M, V)$ and $p_t = f(t, M, V)$. Holding time is determined by the relation $p_{1\_\max} = f(T_H, M, V)$. Solve the above equations for T_H leads to $T_H = f(M, V)$. Thus vacuum holding time T_H depends on both the volume of depressurization chamber and the volume ratio *M* of the test and depressurization chambers. Figure 5.4 shows this relationship for different values of *M* and *V*.

It is clear that, at certain setting level of vacuum pressure regulator D-51, vacuum holding time is proportional to the volume ratio *M*. If the volume of both the test chamber and the depressurization chambers are changed together to maintain the same ratio, then

such a change has little influence on the holding time. In general, volume ratio *M* is the main factor in determining the vacuum holding time T_H .

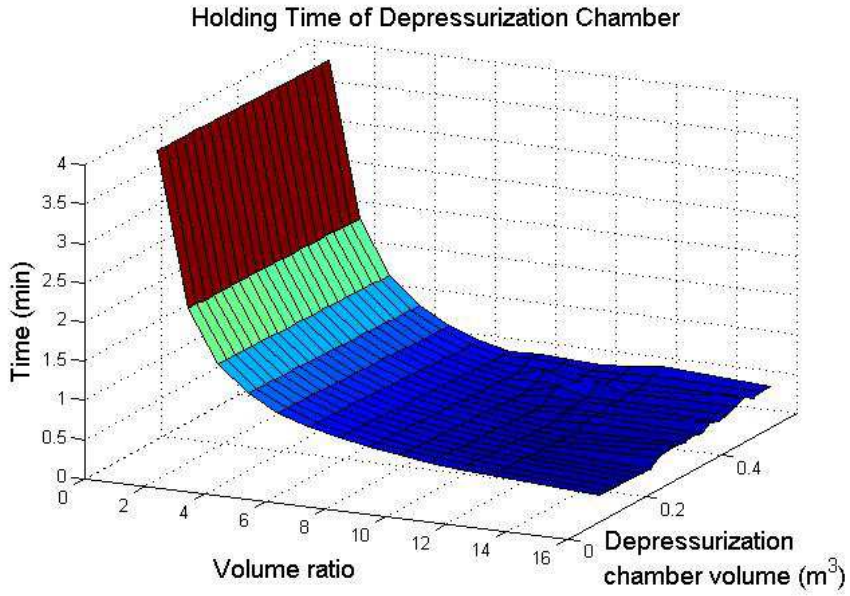

Figure 5.4 Relationship between vacuum holding time and chamber volumes.

Calculation for three specific cases is conducted to show the effect of volume ratio *M* on the pressure and flow rate in both the test chamber and the depressurization chamber. The volume of the depressurization chamber is the same, V_1=0.11149 m^3 (3.9372 ft^3), for all three cases, where M equals to 1, 8 and 15.625, respectively. The result of M = 1 is shown in Figure 4.18, which represents the test chamber and the depressurization chamber at laboratory scaled experiment system.

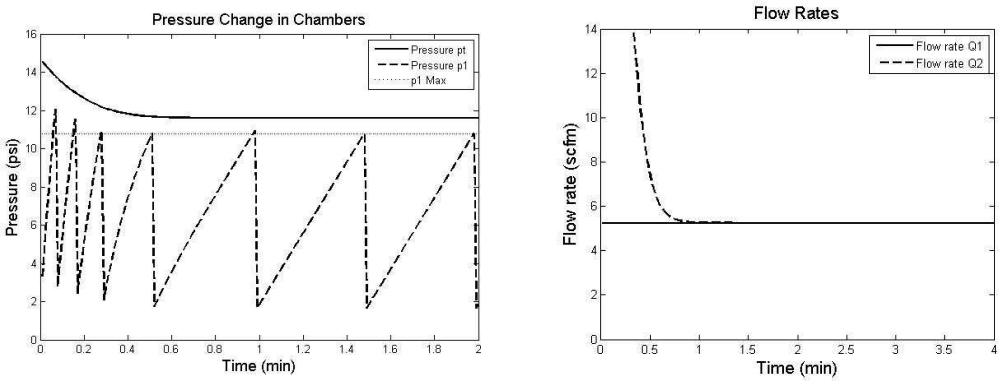

Figure 5.5 Pressures and flow rates at volume ratio $M = 8$.

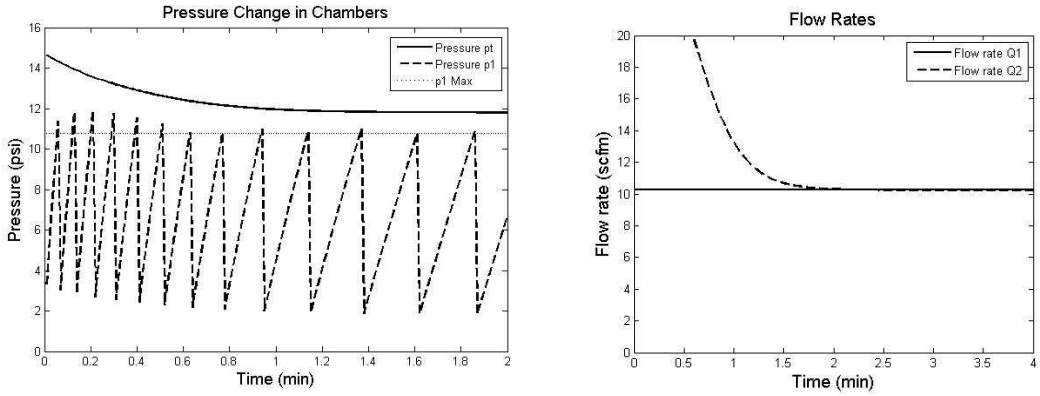

Figure 5.6 Pressures and flow rates at volume ratio $M = 15.625$.

Similarly, calculations are done in the case that the volume of depressurization chamber raises to 7.8745 ft^3, which is twice as the above discussion. The results are summarized in Table 5.1.

Table 5.1 Summary for Vacuum Holding Time

V (ft^3)	**V_1:V Ratio M**	**Flow rate Q_1 = Q_2 (ft^3/min)**	***Pressure p_t (psi)**	****Holding time (min)**
3.9372	1	0.6562	11.4519	4.05
3.9372	8	5.2496	11.6007	0.50 (30 seconds)
3.9372	15.625	10.2531	11.8022	0.26 (15.6 seconds)
7.8745	0.5	0.6562	11.4519	8.09
7.8745	4	5.2496	11.6007	1.00
7.8745	7.8125	10.2531	11.8022	0.51 (30.6 seconds)

* Setting pressure of vacuum regulator is 8.10×10^4 Pa (6" Hg vacuum = 11.7522 psi).
** Holding time is recorded once $p_1(T_H) > 7.42\times10^4$ Pa (10.76 psi=0.73 atm) when the system works continuously (without the initial effect).

The results in Table 5.1 are consistent with the relation shows in Figure 5.4, which further prove the conclusion that vacuum holding time is proportional to the volume ratio of test chamber and depressurization chamber.

5.2.2 The Influence of Volume to Vacuum Generating Time

The volume influence on the vacuum generating time, including steam filling time, cooling time and transition time, is mainly determined by the depressurization chamber.

By adjusting the volume setting in the model discussed in Section 4.1, the relationship between the volume of the depressurization chamber and the steam filling time could be obtained, as shown in Figure 5.7. The result shows that this is almost a linear relation.

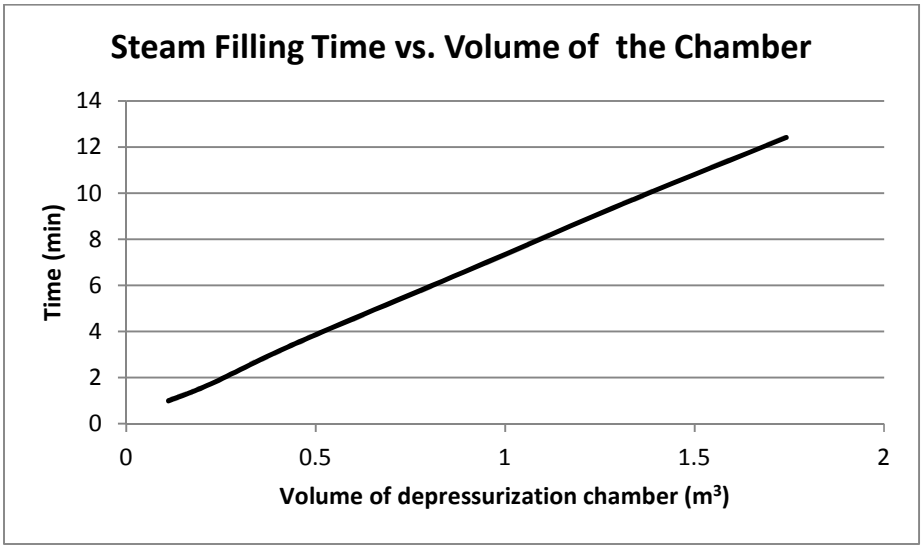

Figure 5.7 Relationship between steam filling time and the volume of depressurization chamber.

The cooling time is considered based on the prediction models discussed in Section 4.2. With the volume raise of the depressurization chamber, the cooling time changes as shown in Figure 5.8.

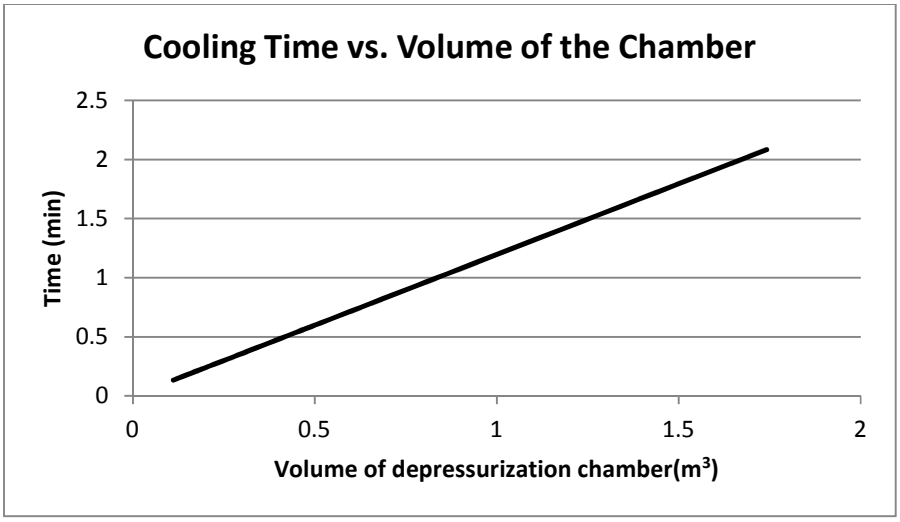

Figure 5.8 Relationship between cooling time and the volume of the depressurization chamber.

The transition time is quite small, comparing with the steam filling time and cooling time. An additional 5% time is added to the sum of steam filling time and cooling time as an estimation of the transition time. So, the relationship of vacuum generating time and volume of the depressurization chamber can be summarized as in Figure 5.9.

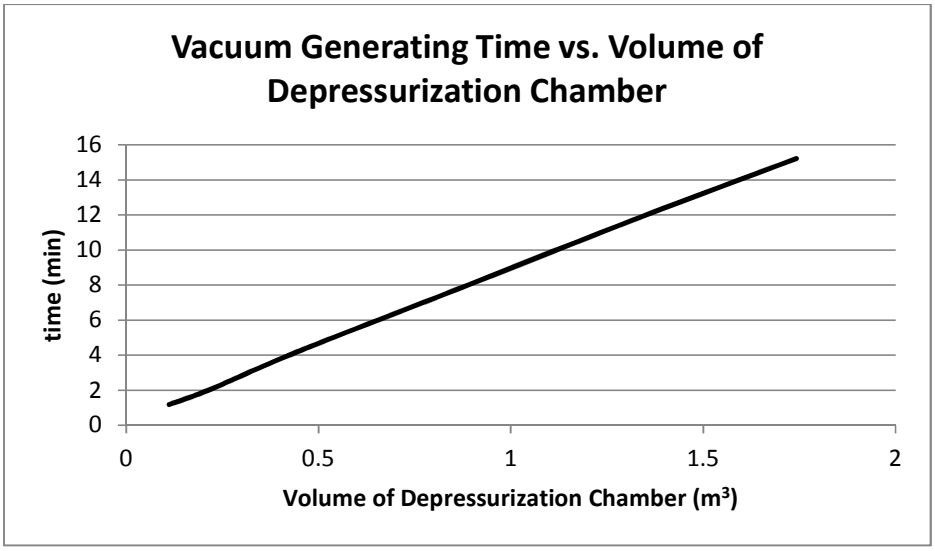

Figure 5.9 Relationship between vacuum generating time and the volume of depressurization chamber.

Considering both the vacuum generating and vacuum holding time with the change of the volumes of test chamber and depressurization chamber, it can be found that with the given volume setting of the test chamber, the raise of the depressurization chamber will increase the vacuum holding time while also increase the steam generating time. The optimal volume design for the depressurization chambers should be determined in every specific case based on the above analysis.

5.3 Elimination of the Transition Phase

As discussed in Chapter 4, a transition phase is used in order to avoid the water used for steam generation flows into the depressurization chambers. If the steam is supplied not by heating the water, this process can be ignored. The most benefits for bypassing the transition phase is that it may accelerate the steam filling speed since at the end of usage phase, the pressure of the depressurization chamber is still less than the atmosphere temperature. And further, the vacuum generating time will be decreased by ignoring the transition phase. This guess is approved by using the modeling in the Section 4.1 and the results are shown as follow.

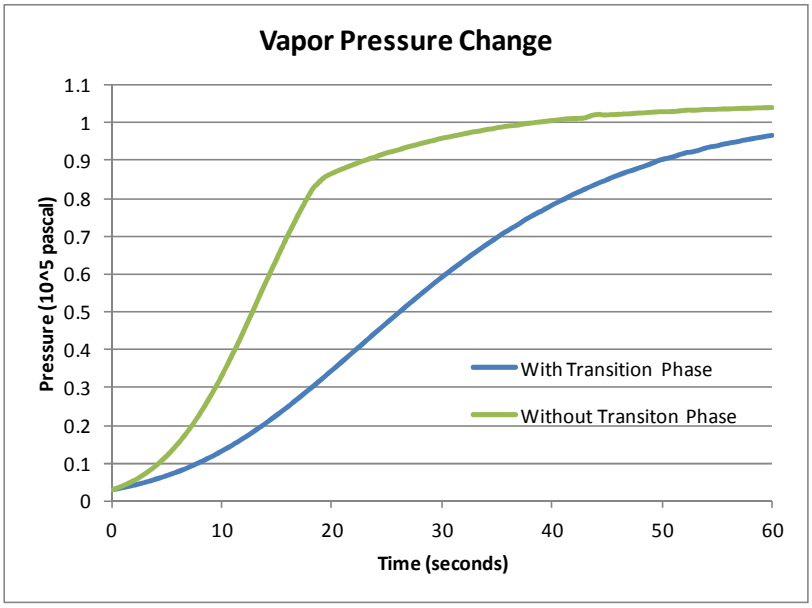

Figure 5.10 Vapor pressure change comparison with and without the transition phase.

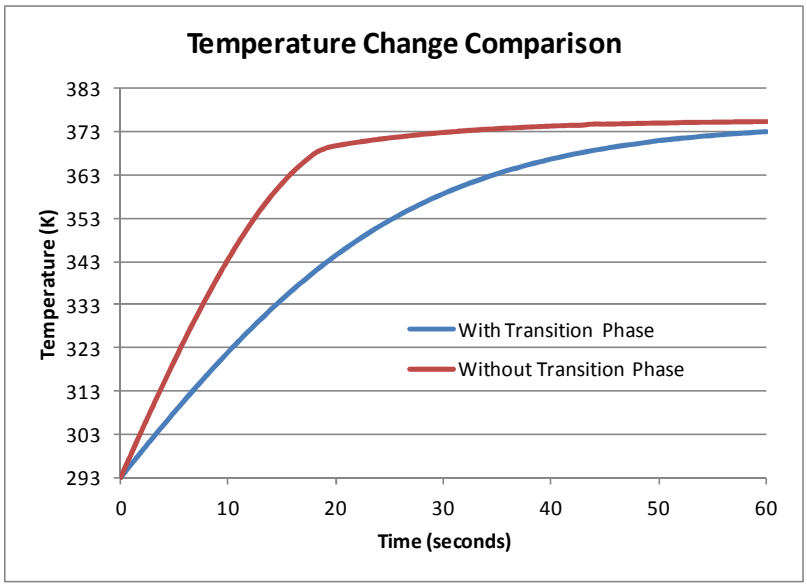

Figure 5.11 Temperature comparison with and without the transition phase.

Figures 5.10 and 5.11 show the vapor pressure change and temperature change with and without transition phase in the steam filling process. The inlet steam is at about 1.05 atm and the volume is the depressurization chamber in the experiment. It is clear that without the transition phase, the steam filling speed is obviously faster, about 30 seconds to reach the 373 K. While for the process with the transition phase, it cost about 55 seconds for the tank temperature to reach the 373K.

5.4 Application to the General Industry Use

The improved vacuum generating techniques discussed above is aimed to be used in general industry applications. According to the requirements of specific application cases, various open circulated vacuum generation and usage systems could be designed. The specifications include the vacuum level of the vacuum chamber, volume of the chamber,

temperature range and gas composition requirements inside the chamber, the maximum or average gas circulate flow rate (vacuum usage rate) and continuous operation time, etc.

With the list of the specification, this condensation based vacuum generation and usage system will be specifically designed. The steam filling factors will be chosen, including the pressure of the source saturated steam and control valve which regulate the filling speed. The pattern of the cooling will be determined. The structure and volume of the depressurization chambers will be chosen to meet the high efficient performance of the system. Other control elements will further decided as well, e.g., the size of the control valves, the process monitor gages and the safety related issues, etc. Figure 5.12 below shows the design chart for the general application.

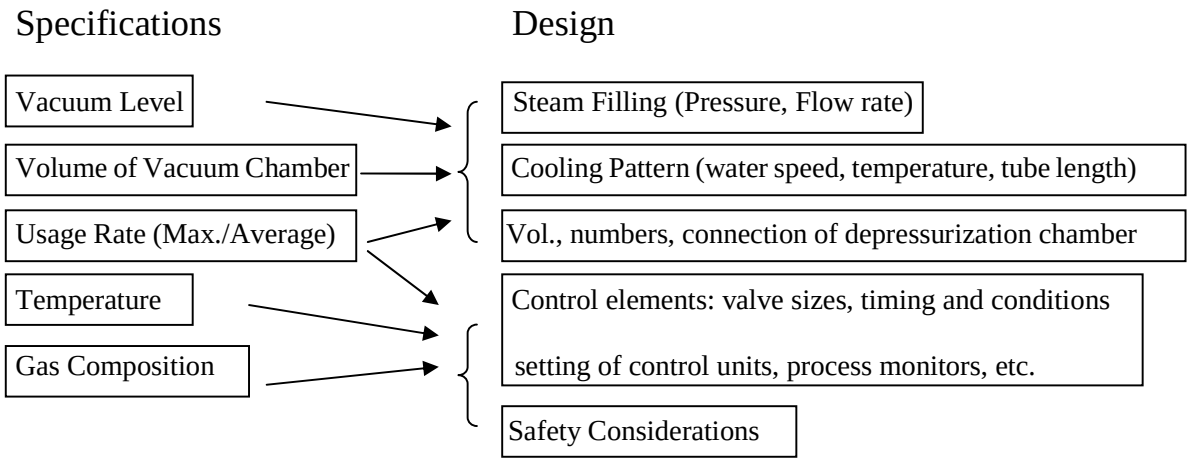

Figure 5.12 Design chart for general applications.

There are several advantages of this vacuum system when used in the industry applications. Using depressurization through steam condensation, the system provides fast, clean and highly efficient vacuum generation. Also the structure of the system is designed to be flexible to meet the wide range of industry requirements. The system exchanges air

with hypobaric chamber with one or more vacuum chambers, according to the need, to maintain the required pressure in the hypobaric chamber. The vacuum level could be adjusted as needed from below 1 atm to about 0.3 atm. The usage rate could be applied from 0.1 ft^3/min to 100 ft^3/min. Finally, when the steam can be provided by the byproduct of the industry, the system is highly sustainable in energy.

CHAPTER 6

CONLUSIONS AND FUTURE WORK

This study designed an automated operation of an experimental vacuum generation system, which is based on the condensation-induced depressurization with prefilled condensable medium in a confined, adiabatic chamber. The control system is implemented on the lab scaled experimental system and achieved its continuously operation. The results of this study can be used to provide industry with a vacuum generation approach which is efficient, without leakage, without moving parts and flexible to the scales change. Modeling and analysis of each of the processing phases provide useful information for the improvement of system performance to the future general applications in industry. Guidelines for designing the vacuum generation systems based on application-specific demand are also presented.

The proposed future work for this study mainly includes three areas. First, a mixing model of the air and steam in depressurization chamber during steam filling phase is needed to replace the current perfect mixing assumption. This model can be used to improve the calculation of steam filling time. Second, the cooling method, which is essential to the depressurization process, will be further studied to enhance the cooling efficiency. Third, improvement of the steam filling phase is needed to reduce the waste of steam at the outlet of the depressurization chamber(s). Approach to reuse the outlet mixture is being studied. Work is already underway in this area and is not included in this dissertation report.

APPENDIX A

LADDER LOGIC DIAGRAM FOR THE IMPLEMENTED CONTROL SYSTEM

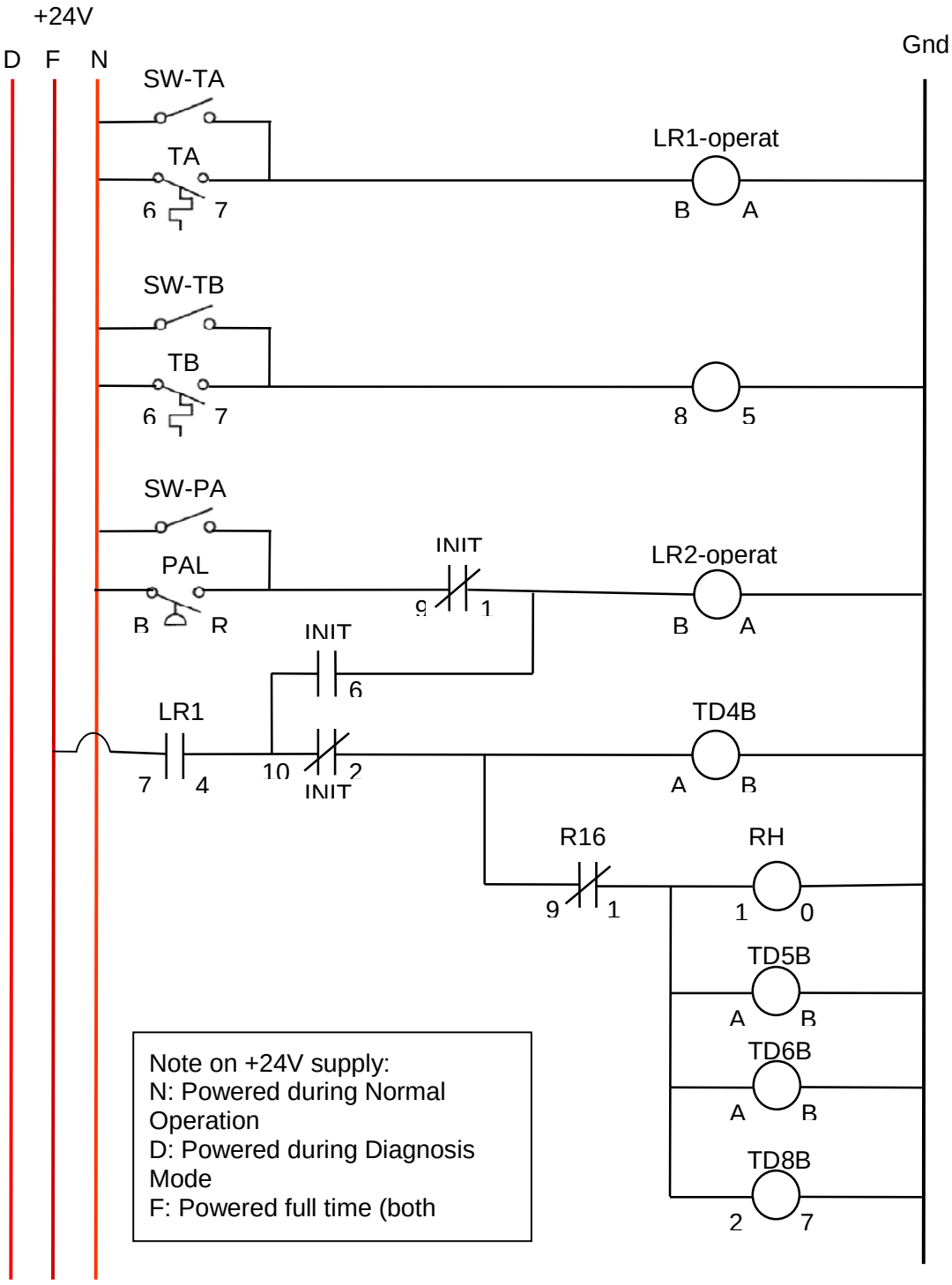

Figure A.1 Ladder logic diagram for the experimental system (to be continued).

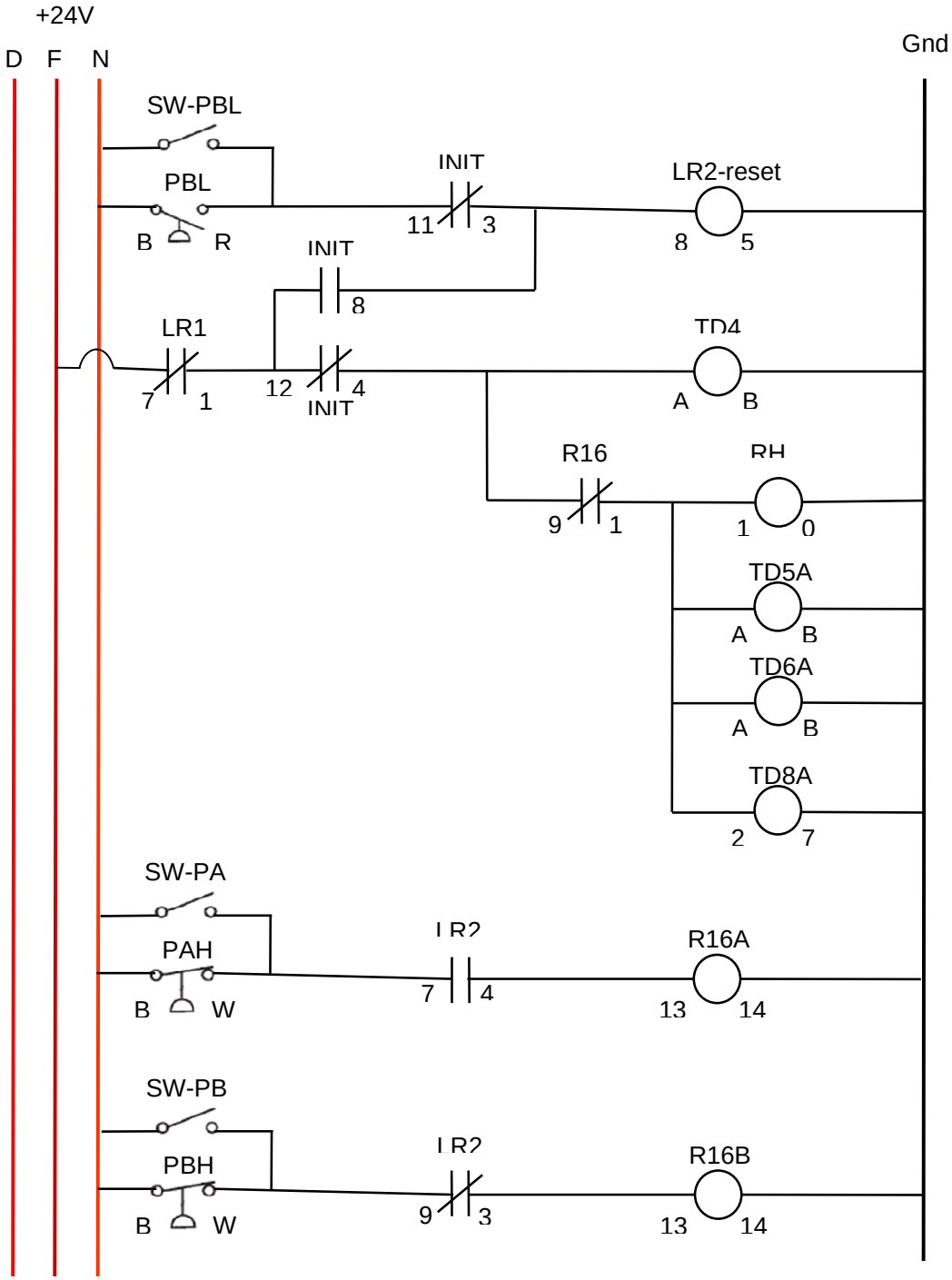

Figure A.1 Ladder logic diagram for the experimental system (to be continued).

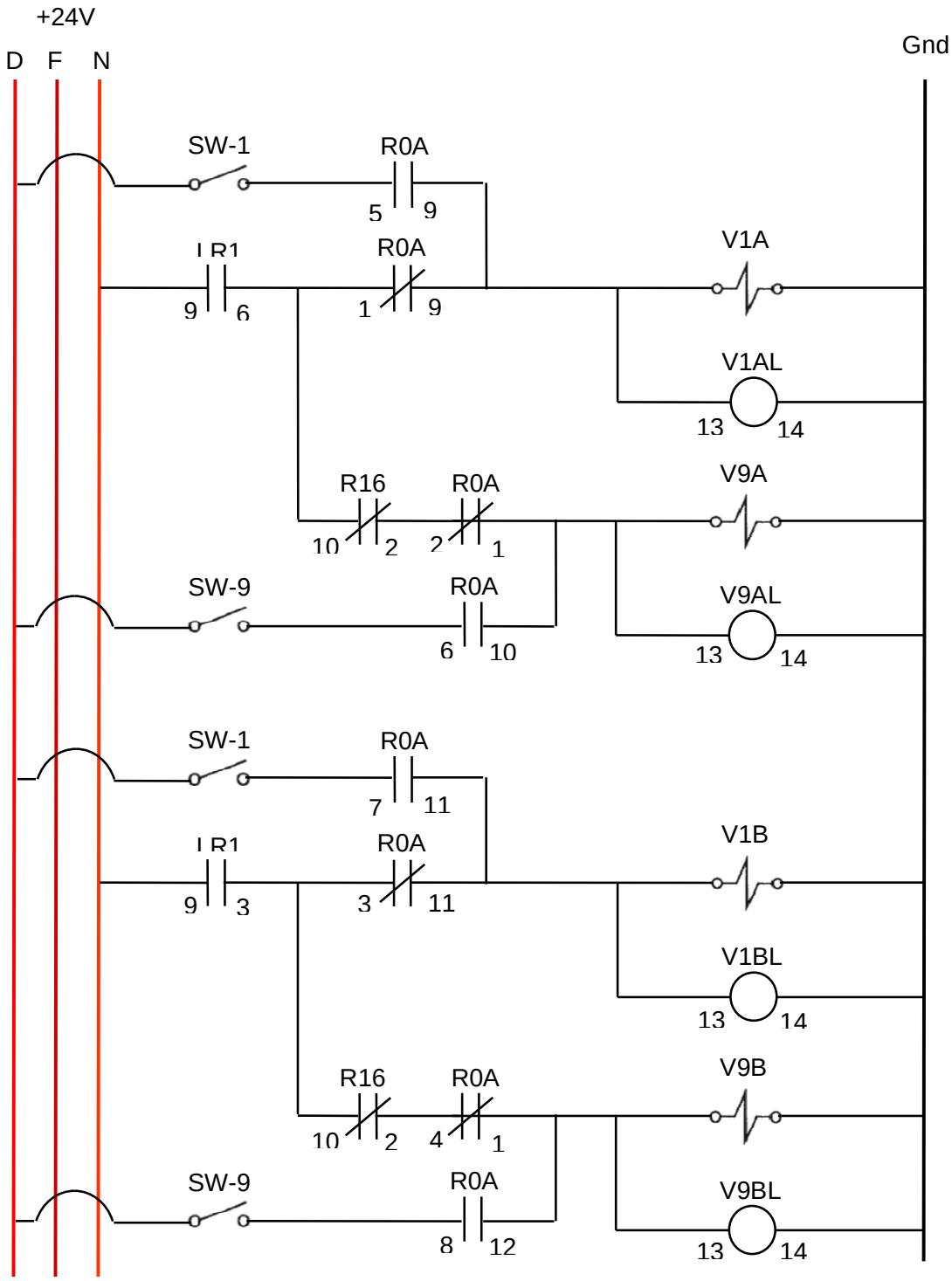

Figure A.1 Ladder logic diagram for the experimental system (to be continued).

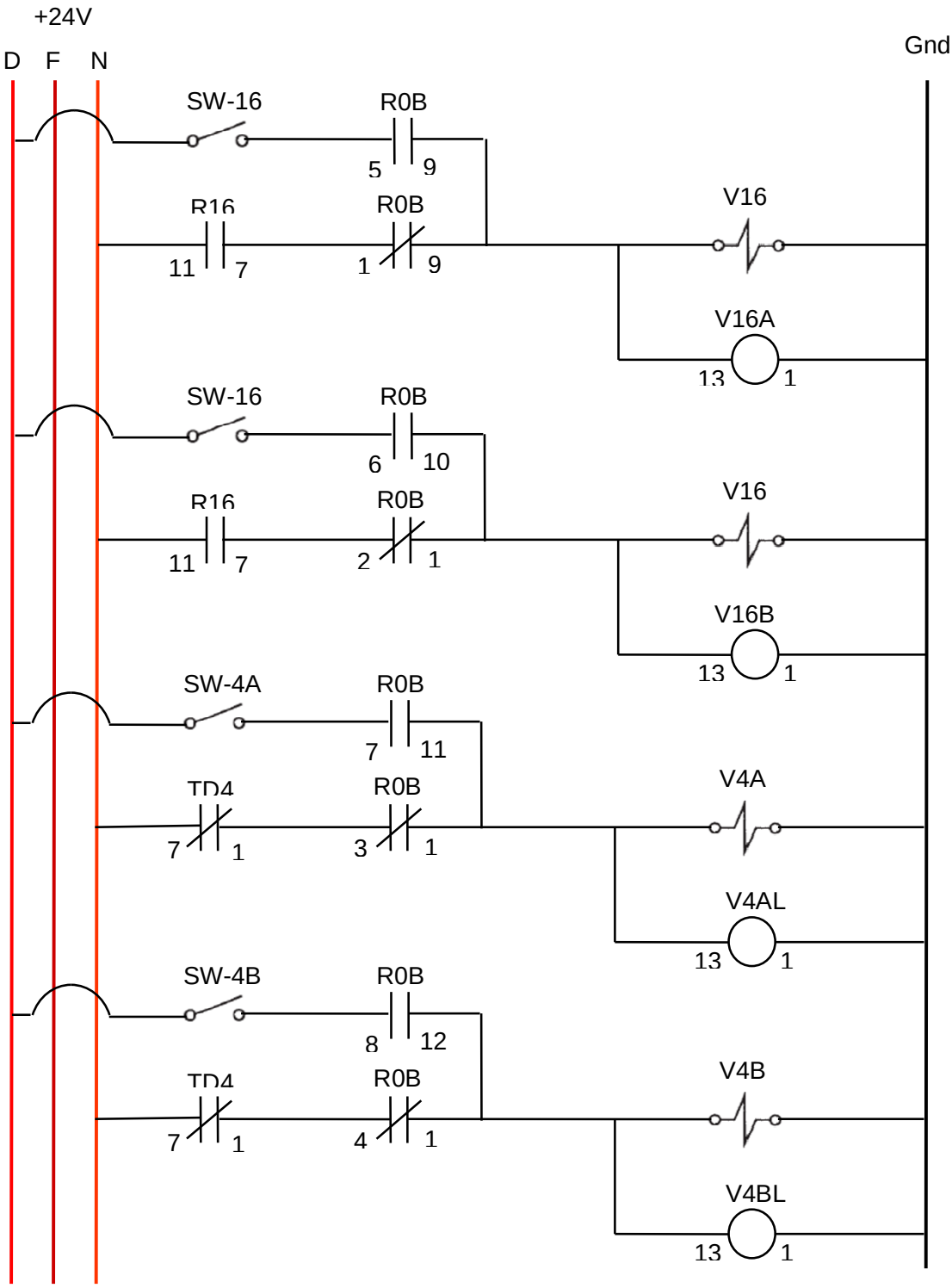

Figure A.1 Ladder logic diagram for the experimental system (to be continued).

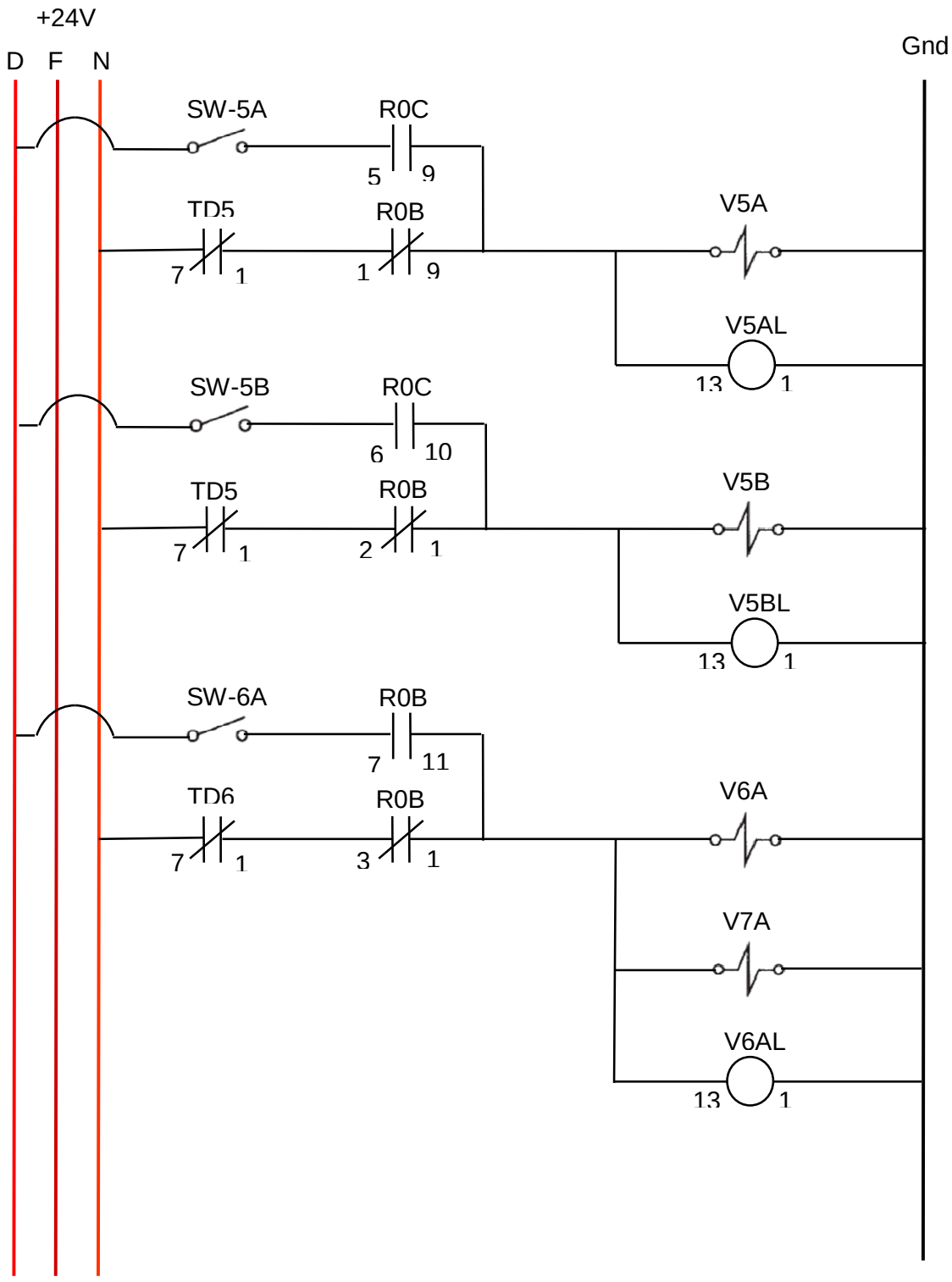

Figure A.1 Ladder logic diagram for the experimental system (to be continued).

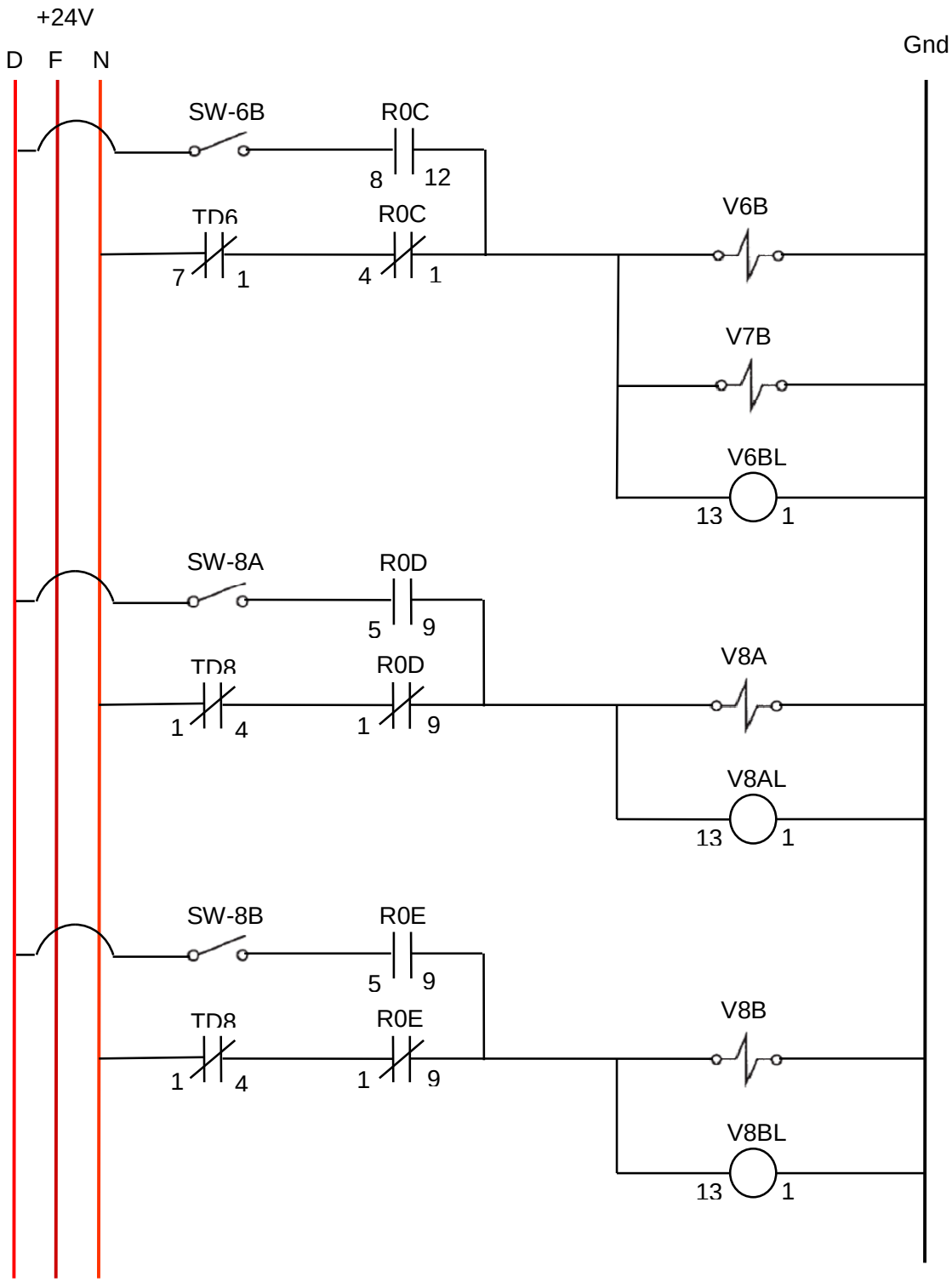

Figure A.1 Ladder logic diagram for the experimental system (to be continued).

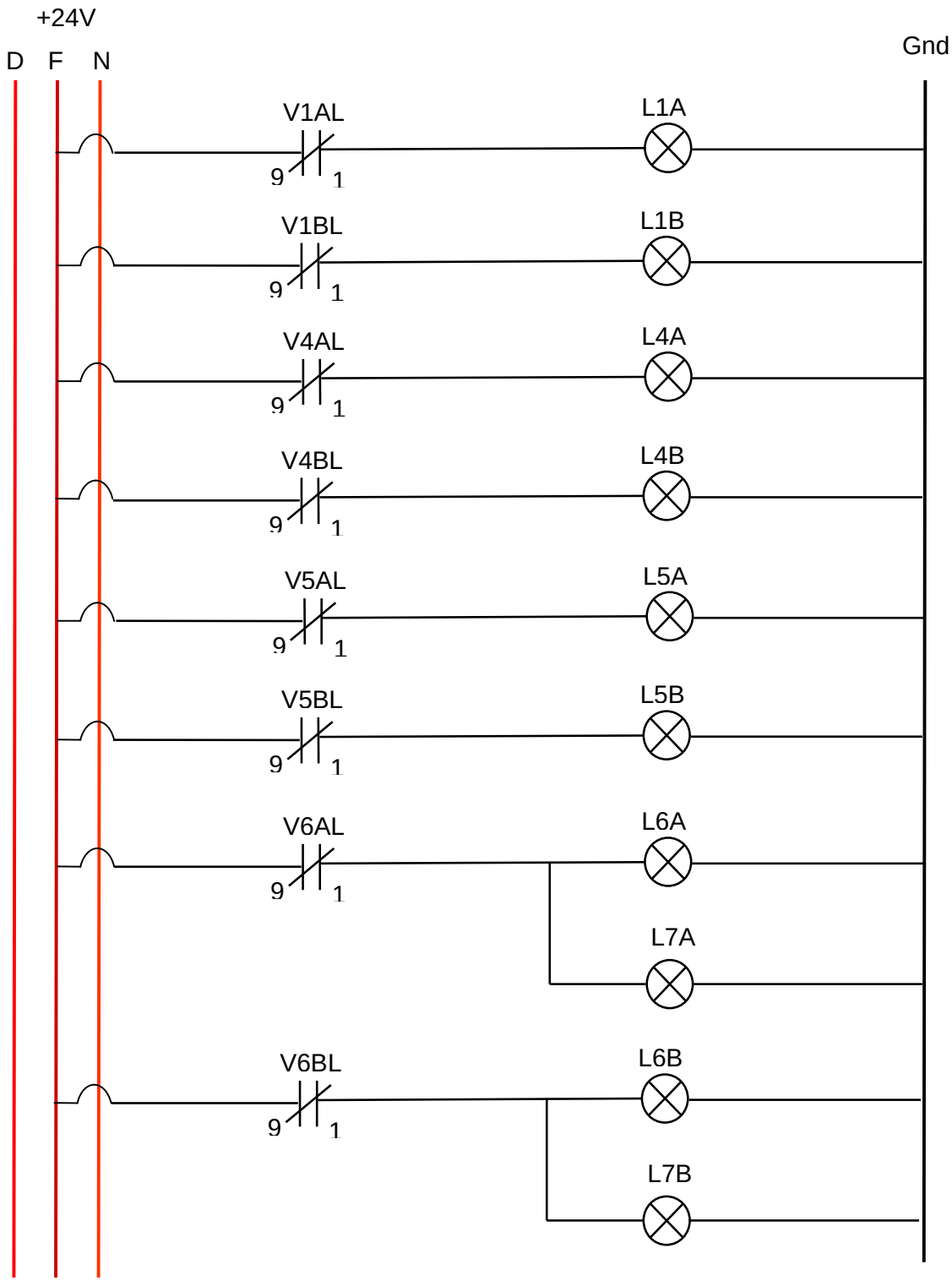

Figure A.1 Ladder logic diagram for the experimental system (to be continued).

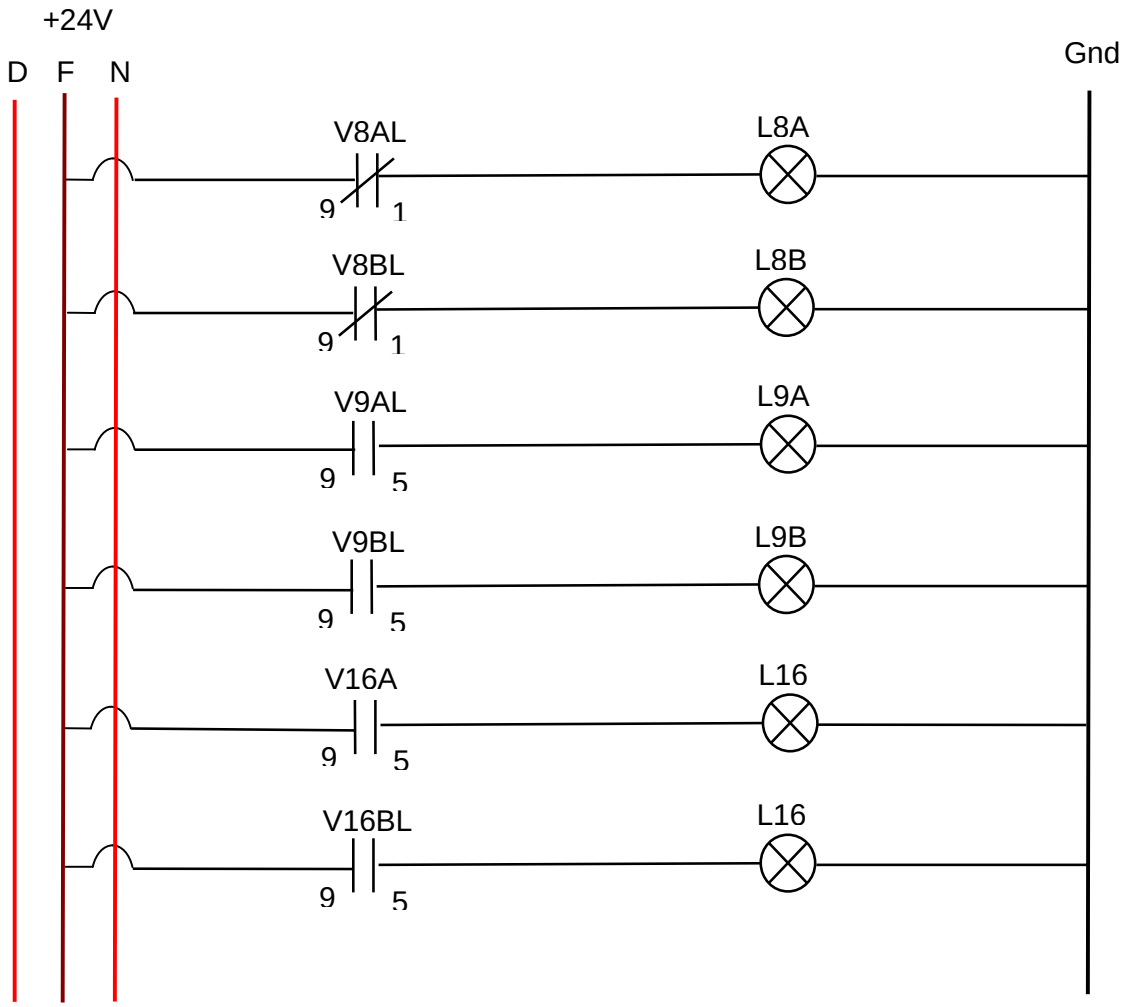

Figure A.1 Ladder logic diagram for the experimental system (to be continued).

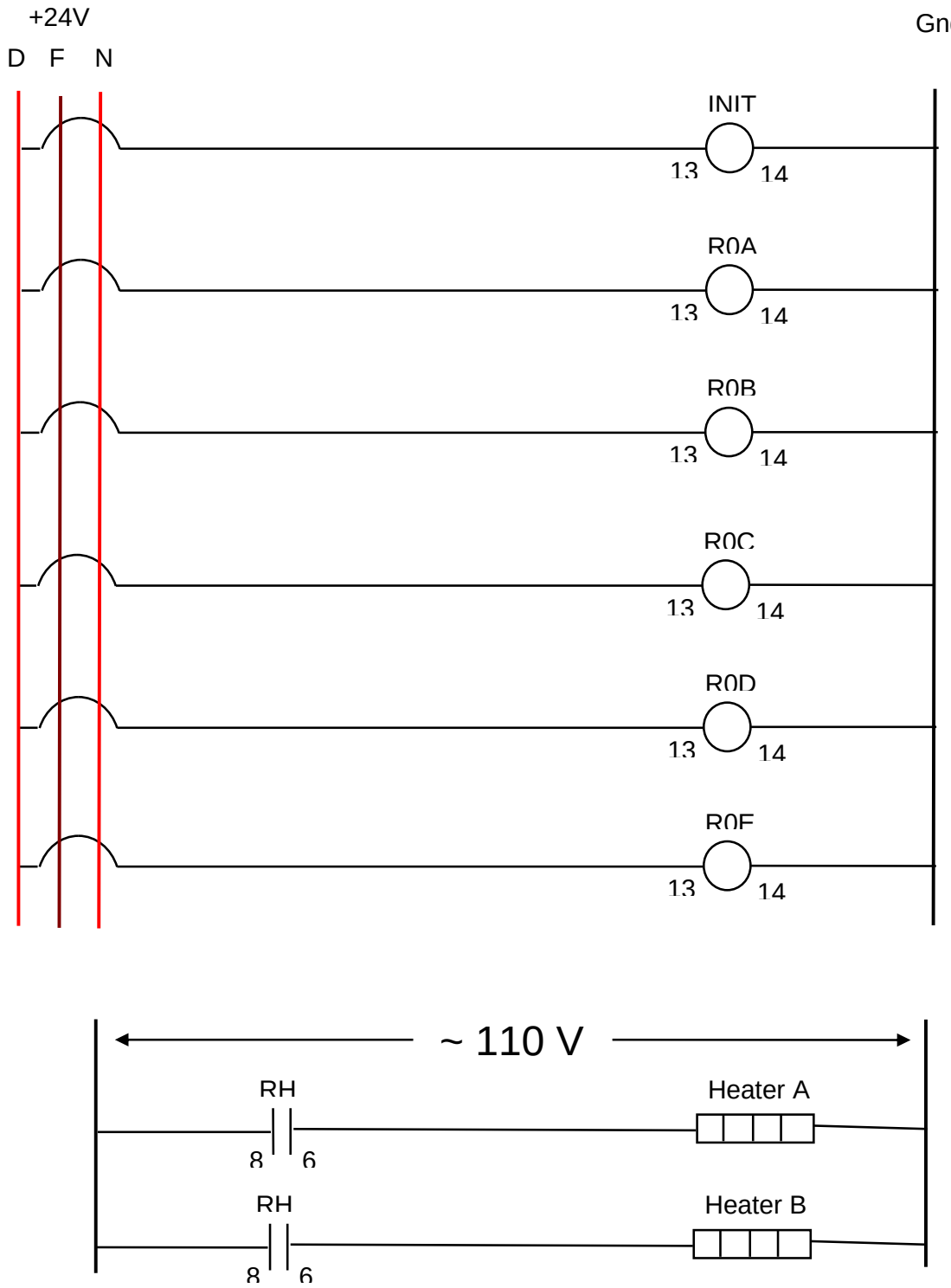

Figure A.1 Ladder logic diagram for the experimental system.

APPENDIX B

VACUUM REGULATOR D-51 CAPABILITY CURVE

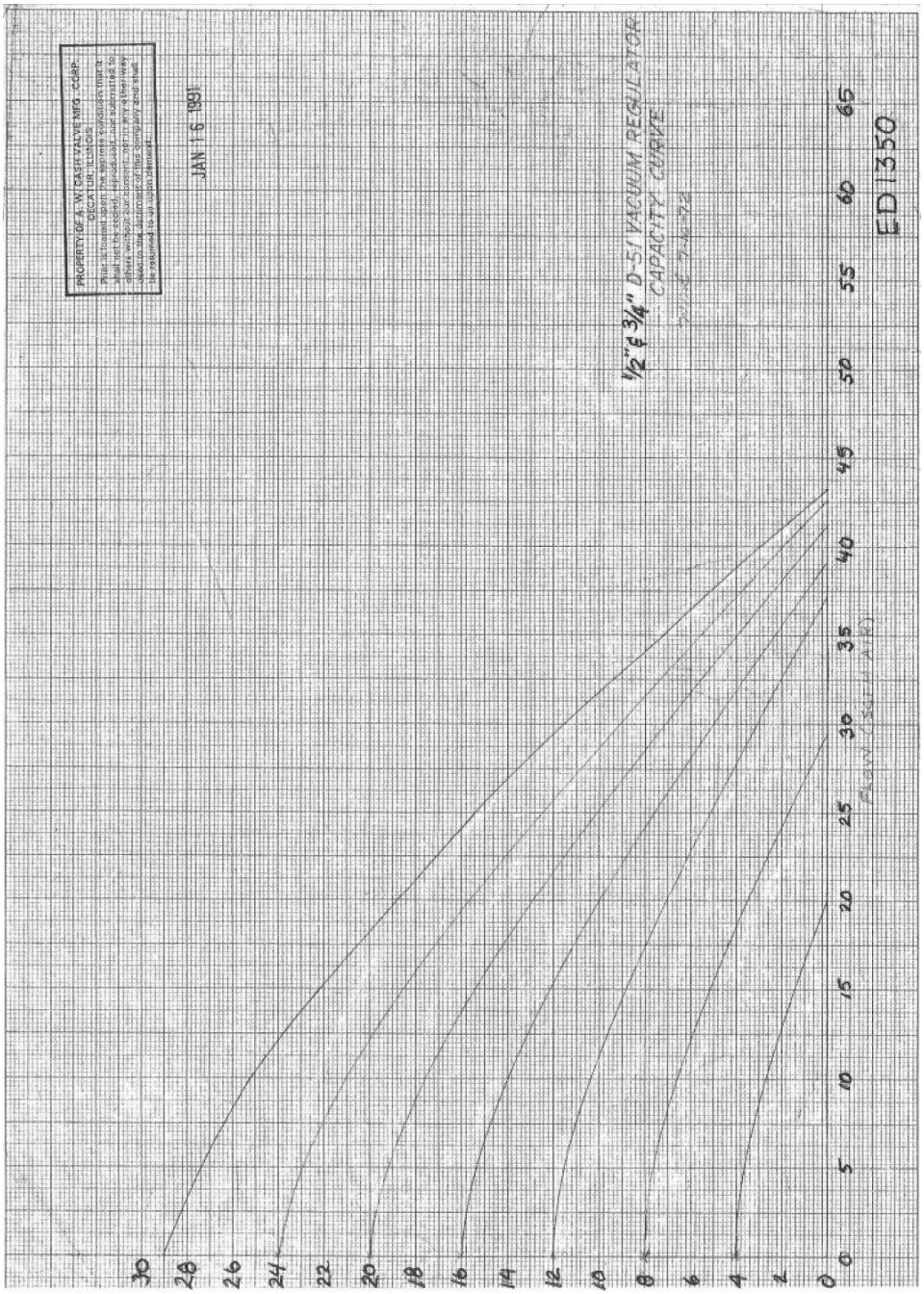

Figure A.2 Capacity curve of vacuum regulator D-51 [30].

REFERENCES

[1] Dubs, Martin, "Coating Chamber, Accompanying Substrate Carrier, Vacuum Evaporation and Coating Methods", U.S. Patent 5,738,729, Apr. 14, 1998 assignor to Balzers Aktiengesellschaft, Furstentum, Liechtenstein.

[2] Löwener Vacuumservice AB Company Vacuum System, from the World Wide Web: http://www.lowener.se/e/vacuum%20systems.htm, accessed on Nov. 5th, 2011.

[3] Hsu, Tai-Ran, ed., *MEMS Package*, p.103-108, INSPEC, The Institute of Electrical Engineers, London, United Kingdom, 2004, ISBN:0-86341-335-8.

[4] Yam, Kit L., ed., *Wiley Encyclopedia of Packaging Technology*, 3rd edition, p.1259-1266, John Wiley & Sons, Hoboken, NJ, 2009, ISBN: 978-0-470-08704-6.

[5] Leskovsek, V., Kalin. M., and Vizintin, J., "Influence of Deep-cryogenic Treatment on Wear Resistance of Vacuum Heat-treated HSS", *Vacuum*, 2006, Vol. 80, p.507-518

[6] Yu, Min, Li, Wen-Ya, Zhang, Chao, and Liao Hanlin, "Effects of Vacuum Heat Treatment on Tensile Strength and Fracture Performance of Cold-sprayed Cu-4Cr-2Nb Coatings", *Applied Surface Science*, 2011, Vol. 257, p.5972-5976.

[7] Schwartz, Mel M., *Brazing*, 2nd edition, p.28-31, ASM International, Material Park, OH, 2003, ISBN: 0-87170-784-5.

[8] Groover, Mikell P., *Fundamentals of Modern Manufacturing: Materials, Processes, and Systems*, 4th edition, p.751-763, John Wiley & Sons, Hoboken, NJ, 2010, ISBN: 978-0470-467008

[9] Sun, Da-Wen and Wang, Lijun, "Heat Transfer Characteristics of Cooked Meats Using Different Cooling Methods", *International Journal of Refrigeration*, 2000, Vol. 23, 7, p.508-516.

[10] Brosnan, Tadhg. and Sun, Da-wen, "Precooling Technique and Applications for Horticultural Products—A Review", *International Journal of Refrigeration*, 2001, Vol. 24, 2, p.154-170.

[11] Vacuum leaks testing, Wikipedia, the free encyclopedia, File:Vacuum Chamber Package testing, from the World Wide Web: http://en.wikipedia.org/wiki/File:Vacuum_Chamber_Package_testing.jpg, accessed on Oct. 18th, 2011.

[12] Jackson, Randal, "Tiny Measurement Gives Big Boost to Planet Hunt", PlanetQuest, from the World Wide Web: http://www.nasa.gov/vision/universe/newworlds/mam-testbed_prt.htm, accessed on Oct. 20th , 2011.

[13] Hoffman, Carl, "Trains- Atlantic Maglec Vacuum Tube Train", *Popular Science*, April, 2004.

[14] Hunt, Elwood H. and Space, David R., "The Airplane Cabin Environment: Issues Pertaining to Flight Attendant Comfort", International In-flight Service Management Organization Conference, Montreal, Canada, p. 1, Nov. 1994.

[15] Hunt, Elwood H., Reid, Don H., Space, David R., and Tilton, Fred E., "Commercial Airliner Environmental Control system—Engineering aspects of cabin air quality", from World Wide Web: www.**cabin**files.com/?CFrequest=file;03032001100119, accessed on Nov. 19th, 2011.

[16] Noller, H.G., Vide, L., "Method for Producing and Measuring A Vacuum", *Vacuum*, 1963, Vol.13, 7, p. 283.

[17] Anon, "High Vacuum by Condensation", *Vacuum*, 1963, Vol. 13, 1, p. 17.

[18] Thiel, A., "Principles of Vacuum Forming", *Vacuum*, 1966, Vol. 16, 3, p. 149.

[19] Junge. H., "Sorption and Condensation as the Basic Principle of New Vacuum Pumps", *Vacuum*, 1967, Vol. 17, 4, p. 247.

[20] Weston, G. F., "Pumps for Ultra-high Vacuum", *Vacuum*, 1978, Vol. 28, 5, p. 209-233.

[21] Van Atta, C. M., Hablanian, M., eds, Vacuum and Vacuum Technology, Encyclopedia of Physics, 2nd edition

[22] O'Hanlon, John F., *A user's guide to vacuum technology*, 3rd edition, p.181-182, John Wiley & Sons, Hoboken, NJ, 2003, ISBN: 0-471-27052-0

[23] He, Pengfei, Patel, Rajesh and Zhu, Chao, Cooling-induced Depressurization of a Steam-filled Chamber, the ASME/JSME 2011 8th Thermal Engineering Joint Conference, March 13-17, 2011, Honolulu, Hawaii, USA, AJTEC2011-44155.

[24] Moran, Michael J. and Shapiro, Howard N., "Fundamentals of Engineering Thermodynamics", 2nd edition, p.695-697, John Wiley & Sons, Inc., New York, 1992, ISBN: 0-471-53984-8.

[25] Young, J. B., "An Equation of State for Steam for Turbomachinery and Other Flow Calculations", *Journal of Engineering for Gas Turbines and Power*, January 1988, Vol. 110, p.1-7.

[26] Branan, Carl R., ed., "Rules of Thumb for Chemical Engineers: A Manual of Quick, Accurate Solutions to Everyday Process Engineering Problems", 4th edition, p. 22-25, Burlington, MA, 2005, ISBN: 0-7506-7856-9.

[27] Sonntag, Richard E. and Borgnakke, Claus, *Introduction to Engineering Thermodynamics*, p.383, John Wiley & Sons, Inc., New York, 2001, ISBN: 0-471-32172-9

[28] Assured Automation,Valve Manual for 101 series, from World Wide Web: http://assuredautomation.com/literature/101_datasheet.pdf, accessed on May 2nd, 2011.

[29] Emerson Electric Co., "Complete Technical Section" from Technical Reference for Regulator, p.591, from World Wide Web: http://www2.emersonprocess.com/en-US/brands/fisherregulators/TechnicalReference/Pages/TechnicalReference.aspx#rct, accessed on November 19th, 2011.

[30] Cash Valve Corp., Manual for Vacuum Regulators and Vacuum Breakers, from World Wide Web: http://www.cashvalve.com/PDF/CAVMC-0523-US.pdf#xml=http://www.searchtycoflowcontrol.com/texis/webinator/search/pdfhi.txt?query=d+51&pr=cash&prox=page&rorder=500&rprox=500&rdfreq=500&rwfreq=500&rlead=500&rdepth=0&sufs=0&order=r&cq=&id=4e2a717a39, accessed on November 21st, 2011.

[31] Cash Valve Corp, ½" and ¾" D-51 Vacuum Regulator Capacity Curve,1991.

[32] Butcher, John Charles, *Numerical Methods for Ordinary Differential Equations*, p. 93-104, John Wiley & Sons, Chichester, West Sussex, England, 2008, ISBN: 978-0-470-72335-7.